

RESEARCH
ENGINEERING
PRODUCTION

9/1/63

N64-19985

CODE-1

NASA CR-53509

TECHNICAL REPORT NO. 349

GENERALIZED VISCOUS MULTICOMPONENT-
MULTIPHASE FLOW WITH APPLICATION TO
LAMINAR AND TURBULENT JETS OF HYDROGEN

By
Raymond Edelman
Harold Rosenbaum
Simon Slutsky

OTS PRICE

XEROX

\$

8.60

MICROFILM

\$

2.93

June 5, 1963

GENERAL APPLIED SCIENCE LABORATORIES, INC.
MERRICK and STEWART AVENUES, WESTBURY, L.I., N.Y. • (516) ED 3-6960

597-10166

TECHNICAL REPORT NO. 349

GENERALIZED VISCOUS MULTICOMPONENT -
MULTIPHASE FLOW WITH APPLICATION TO
LAMINAR AND TURBULENT JETS OF HYDROGEN

By
Raymond Edelman
Harold Rosenbaum
Simon Slutsky

Prepared for
George C. Marshall Space Flight Center
Huntsville, Alabama
Under Contract No. NAS8-2686

Prepared by
General Applied Science Laboratories, Inc.
Merrick and Stewart Avenues
Westbury, L.I., New York

June 5, 1963

Approved By

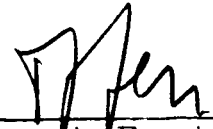

Antonio Ferri
President

TABLE OF CONTENTS

<u>SECTION</u>	<u>TITLE</u>	<u>PAGE</u>
	ABSTRACT	iii
	LIST OF SYMBOLS	iv
I	INTRODUCTION	1
II	ANALYSIS	3
III	CONSTITUTIVE RELATIONS FOR THE RATE PHENOMENA	15
IV	MULTICOMPONENT PHASE EQUILIBRIUM	25
V	APPLICATION TO CHEMICALLY FROZEN AXISYMMETRIC JET IN PHASE EQUILIBRIUM	30
VI	DISCUSSION	41
	REFERENCES	45
	FIGURES	47

ABSTRACT

19985

A

A model is established for the continuum flow of a multicomponent system of gases and their condensed phases. The general conservation equations governing the behavior of the gases and condensed phases are derived. Viscosity, heat conductivity, diffusion and production of species by chemical reactions are included in the development. Non-equilibrium phenomena associated with the presence of condensed phases is discussed in some detail.

Preliminary application to the high altitude hydrogen dumping process is made in an analysis and numerical calculation on a chemically frozen (diffusion controlled) axisymmetric jet in phase equilibrium.

Author

LIST OF SYMBOLS

x	Streamwise coordinate
r	Radial coordinate
p	Pressure
R	Gas constant
T	Temperature
W	molecular Weight
ρ	Mass concentration in mixture
$\dot{\sigma}_v, \dot{\sigma}_l$	Unilateral evaporation and condensation rate, respectively
$\dot{W}_v^F = \dot{\sigma}_v - \dot{\sigma}_l$	Production of gas by evaporation
v	Velocity
h	Static enthalpy
H	Stagnation energy
u	Internal energy
L	heat of phase change
δ	density
\underline{f}	Force of interaction between gas and condensed phases.
\dot{Q}	Heat transfer interaction between gas and condensed phases.
N_p	Droplet number concentration
\dot{W}_v^c	Production of gas by chemical reaction

Y_{vi}	Mass concentration of the i^{th} gaseous species in the gas phase
X_{Pi}	Mass concentration of the i^{th} condensed species in the condensed
β_i	Mass concentration of i^{th} species in the mixture
j_{vi}	Diffusional mass flux defined by equation 12
μ	Viscosity
π	Stress tensor
k	Thermal conductivity
q	Heat flux by conduction
C_D	Drag coefficient defined by Eq. 37a
λ	Heat transfer coefficient defined by Eq. 40a
h_D	Mass transfer coefficient
Re	Reynolds No. ($\frac{\rho v r}{\mu}$)
Pr	Prandtl No. ($\frac{C_p \mu}{k}$)
Le	Lewis No. ($\frac{\rho D C_p}{k}$)
N_u	Nusselt No. defined in eq.'s 50 and 52 for heat and mass transfer, respectively
D_{ii}	Binary diffusion coefficient
A_i', ω_i	Constants in Eq. 57
Ψ	Stream function defined by Eq. 83
ξ	Transformed x coordinate defined by Eq. 85
U	Non-dimensionalized streamwise velocity component

Subscripts

e	Free Stream
j	Jet
i	i th species
p	Particle
g	Gas mixture
v	component in the gas phase
m	Total mixture

GENERALIZED VISCOUS MULTICOMPONENT -
MULTIPHASE FLOW WITH APPLICATION TO
LAMINAR AND TURBULENT JETS OF HYDROGEN

By

Raymond Edelman
Harold Rosenbaum
Simon Slutzky

I. INTRODUCTION

The dumping of combustibles overboard from stages of boost vehicles creates several problems of potential importance. The combustion, surface heating, and induced pressure forces acting on the missile surface are possible consequences of the dumping process. The problem is quite complex owing to the combined effects of finite rate chemistry and jet boundary layer interaction with the external flow. Investigations involving gaseous combustibles under conditions simulating launch trajectories are developed and discussed in Ref. (1, 2, 3, 4).

Common to these investigations is that the various species were present in the gas phase only. However, when cryogenic hydrogen is the fuel under consideration, it becomes necessary to consider the possibility of two-phase flow. In fact, a typical state in the hydrogen fuel tank consists of saturated liquid hydrogen at approximately 20°K ($p \cong 1 \text{ atm}$). Thus, at high altitudes, say of the order of 200,000 feet, it is possible to expand the hydrogen into the solid-vapor region. Furthermore, if the expansion is nearly

isentropic from 40 to 80% of the hydrogen can be in the solid phase (where $T \approx 10^{\circ}\text{K}$) depending on whether vapor or liquid is bled from the tank. It is clear, therefore, that the subsequent mixing with the surrounding air can lead to condensation of the air. In general then, we can expect the flow field to be comprised of the components of air and hydrogen each occurring in two-phases.

The problem of accounting for the effects due to the presence of condensed species can be divided into two parts: (1) development of the conservation equations for the flow field and (2) determination of constitutive relations for the transfer of mass, momentum, and energy between the phases. The first part involves the description of the conservation of mass, momentum, and energy for the gas phase and the condensed phase systems. The second part involves the description of the dynamic and thermodynamic interactions between the gas and condensed phase systems. In general, the second part involves the description of velocity differences between the phases (dynamic non-equilibrium), temperature differences (thermal non-equilibrium), and mass transfer between the phases (non-equilibrium phase changes). This latter process comes under the heading of condensation-evaporation kinetics.

The purpose of the present report is to provide a model from which a system of governing equations may be deduced and to indicate constitutive relations which may be used to account for the interaction phenomena. Finally, the results of the analysis are applied to special cases which are of present interest.

The authors gratefully acknowledge the useful discussions with Dr. Vito Agosta of the Polytechnic Institute of Brooklyn and Mr. Andrew Pouring of Yale University as well as the numerical calculations carried out by Mr. David Soll and the IBM 709 program written by Mr. Jay Hoffman.

II. ANALYSIS

In establishing a model for the present complex flow system it becomes necessary to make certain assumptions. These assumptions are, in general, made in regard to the nature of the condensed phase system. The basic assumptions are discussed below.

(1) The condensed phase is in the form of a cloud of solid or liquid particles. This assumption is more of a statement of fact evidenced by launch experience and wind tunnel studies relating to condensation of various gases (5).

(2) droplet-droplet interaction is negligible. That is, the condensed phase is assumed to form a dilute suspension in the gas phase.

(3) the volume occupied by the condensed phase is negligible. This is merely a statement of the fact that the mass density of a condensed species is much greater than the mass density of its vapor.

(4) random motion of the particles of condensed phase is assumed negligible. That is, pressure, temperature and transport properties associated with random motion are considered negligible compared with those of the gas phase. The validity of this assumption rests on the condition that the particle size be larger than that of the molecules in the gas phase.

(5) thermal radiation is neglected. The low temperature with which we are concerned implies that thermal radiation will be negligible.

(6) each droplet has a uniform temperature at any instant. That is, conduction (and convection within the droplet in the case of liquid droplets) is negligible. In general, droplet sizes will be small enough to render this assumption valid.

(7) we shall assume that the state of the vapor at the droplet surface corresponds to the droplet temperature and velocity. This assumption is made in order to provide a means of systematically accounting for the condensed phase-gas phase interactions.

(8) surface energy, gravity and electric charge effects are neglected.

In general, the approach will be to develop a system of governing equations which will describe the behavior of the gas phase globally and the condensed species individually. This permits the gases to be treated as a multicomponent diffusing system with chemical reactions in the way previously developed for gaseous systems (see e.g. Ref. 6). On the other hand, the condensed species are treated individually so that the mass, momentum, and thermal interactions can be handled in terms of the best available information for flow about bodies under the conditions which can prevail in the present investigation. We refer to these relations as the constitutive relations. A discussion of these relations will be taken up after the general conservation equations are derived.

In accordance with assumption (7), each droplet may be thought to have a film of vapor surrounding it. Within this film, velocity and temperature are brought from the gas-phase values to the values at the droplet surface. Since the film is vapor, it is associated with the gas phase but is considered to contain negligible mass. This implies that the instantaneous flow of mass, momentum and energy from the particles is equal to the instantaneous gain of mass, momentum and energy by the gas phase. Thus, the film is the source of irreversible entropy production due to the non-equilibrium transfer of mass, momentum and

energy between the phases. It must be noted that the mass transfer which is due to evaporation and condensation has an associated momentum and energy transfer. These are in addition to the momentum and energy transfers due to velocity and temperature differences, respectively. Let us consider this point in more detail as follows. In the first place, assumption (2) implies that the influence of the condensed phase on the flow field may be constructed in terms of the interactions associated with a single particle and its surroundings multiplied by a local number density of droplets in the elemental volume of mixture. This permits the use of available information for the interaction of single droplets in an infinite fluid. Further, the introduction of the local number density "smears" out the actual discrete nature of droplet system. The result of this is to predict a local, as well as overall, average effect of the droplets on the flow field. We consider first, the mass, momentum and energy transfers with the evaporation and condensation process.

Mass Transfer: The process of evaporation is composed of a simultaneous unilateral evaporation rate, $\dot{\sigma}_v$, and a unilateral condensation rate. The net result of the two unilateral rates is the evaporation rate. Thus, we have:

$$\dot{W}_v^F = \dot{\sigma}_v - \dot{\sigma}_\lambda$$

Clearly, if this difference is negative we have condensation and if it is zero there is, in effect, no phase change.

Momentum: The droplet loses momentum at a rate equal to $\dot{\sigma}_v \underline{V}_p$ and simultaneously gains momentum at a rate equal to $\dot{\sigma}_l \underline{V}_p$. This is in accordance with the condition that at the interface the vapor and droplet have the same velocity \underline{V}_p . Thus, the net loss of droplet momentum is given by:

$$\underline{V}_p (\dot{\sigma}_v - \dot{\sigma}_l) = \underline{V}_p \dot{W}_v^F \quad 2$$

This represents a gain in gas phase momentum due to evaporation.

Energy: The droplet energy loss associated with the unilateral evaporation rate is composed of condensed phase enthalpy, kinetic energy, and the heat of vaporization. The gain of droplet energy associated with the unilateral condensation rate is composed of the vapor enthalpy and kinetic energy evaluated at the interface state. Thus, the net loss of droplet energy is given by:

$$\begin{aligned} \dot{\sigma}_v \left(h_p + L + \frac{\underline{V}_p \cdot \underline{V}_p}{2} \right) - \dot{\sigma}_l \left(h_{v_{Tp}} + \frac{\underline{V}_p \cdot \underline{V}_p}{2} \right) &= \\ &= \dot{W}_v^F \left(h_p + L + \frac{\underline{V}_p \cdot \underline{V}_p}{2} \right) \end{aligned} \quad 3$$

Note that the droplet gives up the heat of vaporization and gains the heat of condensation where:

$$h_{v_{Tp}} = h_p + L \quad 4$$

In addition, the interface moves in accordance with the rate of evaporation of the droplet. This results in a work transfer given by:

$$P_p / \dot{\sigma}_l \dot{W}_v^F \quad 5$$

where,

P_p \equiv interface pressure

δ_L \equiv droplet density

$\frac{\dot{W}_L^F}{\delta_L}$ \equiv rate of increase in gas phase volume due to droplet evaporation

Since, in general, $L \gg P_p / \delta_L$, the energy associated with Eq. 5 is negligible compared with that given by Eq. 3.

It has been pointed out that in addition to mass, momentum, and energy transfers associated with evaporation, there exist dynamic and thermal interactions in virtue of the velocity and temperature non-equilibrium between the phases, respectively. These are discussed, in order, in the following.

Drag Force :

The drag force constitutes a momentum interchange between the phases. We shall assume that this force is purely a viscous phenomenon and depends only on the velocity difference, i.e.:

$$\underline{f}_p = \underline{f}_p(\underline{v}_g - \underline{v}_p)$$

6

Additional forces exist but can be shown to be, in general, of higher order (Ref. 7).

Thermal Interaction:

This thermal interaction which is dependent on the temperature difference between the phases is merely a statement of convective heat transfer.

This precludes the existence of radiation heat transfer in accordance with assumption (5). This convective heat transfer is expressed by:

$$\dot{Q}_P = \dot{Q}_P(T_V - T_P)$$

7

In constructing the conservation equations, we shall consider the existence of chemical reactions and assume that these take place in the gas phase.

Conservation Equations:

In consideration of the above discussion, we are now in position to write down the conservation equations in a systematic manner.

In order to maintain generality, we consider i gaseous species and i condensed species i.e. each component can exist in each phase. We consider each condensed species individually. The implication of this treatment of the condensed phase is discussed in a later section dealing with phase equilibrium of multicomponent systems but does not influence the following development.

Continuity of Mass:

For the i^{th} gaseous species:

$$\nabla \cdot \rho_{Vi} \underline{V}_{Vi} = \dot{W}_{Vi}^F + \dot{W}_{Vi}^C$$

8

Where,

$$\sum_i \dot{W}_{Vi}^C = 0$$

$$\sum_i \dot{W}_{Vi}^F = \text{Net production of gas phase mass due to evaporation}$$

$$\sum_i (\dot{W}_{Vi}^F + \dot{W}_{Pi}^F) = 0$$

For the i^{th} condensed species:

$$\nabla \cdot \rho_i \underline{V}_{pi} = \dot{W}_{pi}^F = -\dot{W}_{vi}^F$$

9

In order that the species in the gaseous phase may be treated in the usual manner we introduce the following barycentric (mass mean) quantities:

$$\rho_g = \sum_i \rho_{vi} \quad 10$$

$$\rho_g \underline{V}_g = \sum_i \rho_{vi} \underline{V}_{vi} \quad 11$$

and

$$\underline{j}_{vi} = \rho_{vi} (\underline{V}_{vi} - \underline{V}_g) \quad 12$$

where we further introduce the gas phase mass fractions given by:

$$Y_{vi} = \frac{\rho_{vi}}{\rho_g} \quad 13$$

where,

$$\sum_i Y_{vi} = 1 \quad 14$$

Introducing the definitions 10 - 13 into Eq. 8 gives:

$$\nabla \cdot \rho_g \underline{V}_g Y_{vi} = \dot{W}_{vi}^F + \dot{W}_{vi}^c - \nabla \cdot \underline{j}_{vi} \quad 15$$

which is the "species conservation" equation for the i^{th} gaseous species. If Eq. 15 is summed over all i gaseous species, noting Eq. 14, we get the "global continuity" equation for the gaseous system:

$$\nabla \cdot \rho_g \underline{V}_g = \sum_i \dot{W}_{vi}^F \quad 16$$

In applying the present analysis it will be convenient to introduce a variable for the condensed phase mass fractions defined by:

$$X_{pi} = \frac{\rho_{pi}}{\rho_p} \quad 17$$

where

$$\rho_p = \sum_i \rho_{pi} \quad 18$$

and

$$\sum_i X_{pi} = 1 \quad 19$$

Thus, Eq. 9 for the continuity of mass for the i^{th} species of the condensed phase:

$$\nabla \cdot \rho_p \underline{V}_{pi} X_{pi} = \dot{W}_{pi}^F \quad 20$$

Momentum:

The global gas-phase momentum equation may be written:

$$\nabla \cdot \sum_i \rho_{vi} \underline{V}_{vi} \underline{V}_{vi} = \nabla \cdot \underline{\pi}_g + \sum_i \left(\sum_j \underline{F}_{ji} \right) \underline{V}_i + \sum_i \dot{W}_{vi}^F \underline{V}_{pi} \quad 21$$

where the summation notation, $\sum_i \left(\sum_j \underline{F}_{ji} \right) \underline{V}_i$, reads, "the force of all j particles acting on the i^{th} gas species summed over all i gas species". In terms of the barycentric quantities Eq. 21 with the aid of Eq. 16 becomes:

$$\rho_g \underline{V}_g \cdot \nabla \underline{V}_g = \nabla \cdot \underline{\pi}_g + \sum_i \left(\sum_j \underline{F}_{ji} \right) \underline{V}_i + \sum_i \dot{W}_{vi}^F (\underline{V}_{pi} - \underline{V}_g) \quad 22$$

The i^{th} condensed-phase momentum equation is given by:

$$\nabla \cdot \rho_{pi} \underline{V}_{pi} \underline{V}_{pi} = \left(\sum_j \underline{V}_{ji} \right) \underline{P}_i + \dot{W}_{pi}^F \underline{V}_{pi} \quad 23$$

which with the aid of Eq. 19 may be written:

$$\rho_{pi} \underline{V}_{pi} \cdot \nabla \underline{V}_{pi} = \left(\sum_j \underline{V}_{ji} \right) \underline{P}_i \quad 24$$

Energy:

The combined gas-phase energy equation in terms of the barycentric quantities is given by:

$$\begin{aligned}
\nabla \cdot \rho_g \left(u_g + \frac{V_g \cdot V_g}{2} \right) V_g &= -\nabla \cdot q_g + \nabla \cdot \pi_g \cdot V_g - \sum_i \nabla \cdot j_{vi} h_{vi} \\
&+ \sum_i \dot{Q}_{(E_i) V_i} + \sum_i \sum_j f_{ij V_i} \cdot V_{pj} \\
&+ \sum_i \dot{W}_{vi}^F \left(h_{pi} + L_i + \frac{V_{pi} \cdot V_{pi}}{2} \right)
\end{aligned}$$

25

the i^{th} condensed-phase energy equation is given by:

$$\begin{aligned}
\nabla \cdot \rho_{pi} \left(u_{pi} + \frac{V_{pi} \cdot V_{pi}}{2} \right) V_{pi} &= f_{(E_{vi}) p_i} \cdot V_{pi} + \dot{Q}_{(Z_{vi}) p_i} \\
&- \dot{W}_{vi}^F \left(h_{pi} + L_i + \frac{V_{pi} \cdot V_{pi}}{2} \right)
\end{aligned}$$

26

SUMMARY OF CONSERVATION EQUATIONS:

The equations developed, as initially proposed, govern the mean mass flow field of the gas-phase and the individual flow behavior of the condensed-phase. It is also of interest to consider the "mixture" equations as a possible set of working relations. These equations are obtained by merely summing over all species in all phases. The resulting equations are listed below.

Continuity of Mass:

Mixture:

$$\nabla \cdot (\rho_g V_g + \sum_i \rho_{pi} V_{pi}) = 0$$

27

i^{th} condensed phase:

$$\nabla \cdot \rho_{pi} V_{pi} = \nabla \cdot \rho_p V_{pi} X_{pi} = \dot{W}_{pi}^F = -\dot{W}_{vi}^F$$

28

i^{th} gas phase:

$$\nabla \cdot \rho_g V_g Y_{vi} = \dot{W}_{vi}^F + \dot{W}_{vi}^C - \nabla \cdot j_{vi}$$

29

Momentum

Mixture:

$$\nabla \cdot (\rho_g \underline{V}_g \underline{V}_g + \sum_i \rho_{pi} \underline{V}_{pi} \underline{V}_{pi}) = \nabla \cdot \underline{\Pi}_g \quad 30a$$

or,

$$\rho_g \underline{V}_g \cdot \nabla \underline{V}_g + \sum_i \rho_{pi} \underline{V}_{pi} \cdot \nabla \underline{V}_{pi} = \nabla \cdot \underline{\Pi}_g + \sum_i \dot{W}_{vi}^F (\underline{V}_{pi} - \underline{V}_g) \quad 30b$$

ith condensed phase:

$$\rho_{pi} \underline{V}_{pi} \cdot \nabla \underline{V}_{pi} = f(\sum_j V_j) \rho_i \quad 31$$

Energy

Mixture:

$$\nabla \cdot \left[\rho_g \left(h_g + \frac{\underline{V}_g \cdot \underline{V}_g}{2} \right) \underline{V}_g + \sum_i \rho_{pi} \left(h_{pi} + \frac{\underline{V}_{pi} \cdot \underline{V}_{pi}}{2} \right) \underline{V}_{pi} \right] = \quad 32a$$

$$= -\nabla \cdot \underline{q}_g + \nabla \cdot (\underline{\tau}_g \cdot \underline{V}_g) - \sum_i \nabla \cdot \underline{j}_{vi} h_{vi}$$

or

$$\begin{aligned} & \rho_g \underline{V}_g \cdot \nabla \left(h_g + \frac{\underline{V}_g \cdot \underline{V}_g}{2} \right) + \sum_i \rho_{pi} \underline{V}_{pi} \cdot \nabla \left(h_{pi} + \frac{\underline{V}_{pi} \cdot \underline{V}_{pi}}{2} \right) \\ &= -\nabla \cdot \underline{q}_g + \nabla \cdot (\underline{\tau}_g \cdot \underline{V}_g) - \sum_i \nabla \cdot \underline{j}_{vi} h_{vi} + \\ &+ \sum_i \dot{W}_{vi}^F \left[\left(h_{pi} + \frac{\underline{V}_{pi} \cdot \underline{V}_{pi}}{2} \right) - \left(h_g + \frac{\underline{V}_g \cdot \underline{V}_g}{2} \right) \right] \end{aligned} \quad 32b$$

ith condensed phase:

$$\rho_{pi} \underline{V}_{pi} \cdot \nabla h_{pi} = \dot{Q}(\sum_j V_j) \rho_i - \dot{W}_{vi}^F L_i \quad 33$$

The above relations, 27, 28, 29, 30a or b, 31, 32a or b and 33 constitute seven, 7, partial differential equations for the nine, 9, unknowns:

$$\begin{array}{ll} p_g & s_{pi} \\ \underline{v}_g & \underline{v}_{pi} \\ Y_{vi} & h_{pi} \\ h_g & \\ p_g & \\ h_{vi} & \end{array}$$

The additional relations are supplied by Eq.'s of state:

$$p_g = p_g(p_g, T_g, Y_{vi}) \quad 34$$

$$h_g = \sum_i Y_{vi} h_{vi}(T_g) \quad 35$$

$$u_{pi} \cong h_{pi}(T_{pi}) \quad 36$$

We note that this discussion assumes knowledge of the dependence of \underline{q}_g , $\underline{\tau}_g$ and \underline{j}_{vi} on the above variables. The discussion of these relations is taken up in the next section where similar relations for gas-phase condensed phase interactions are discussed.

III. CONSTITUTIVE RELATIONS FOR THE RATE PHENOMENA

In order to complete the necessary set of governing equations we must supply relations for \underline{f}_i , \dot{Q}_i , \dot{W}_{v_i} , \underline{q}_g , τ_g , and \underline{j}_{v_i} . There exists no available theory for the description of the above six rate parameters occurring simultaneously. The kinetics of condensation and evaporation itself is not fully understood and forms the basis for many current investigations (Ref. 8). The problem of nucleation, condensation and evaporation, from both molecular and macroscopic approaches is reviewed extensively in Ref. 5. On the basis of available information it has been suggested that a semi-empirical approach would be the most fruitful direction to adopt in the present complex problem.*

* The authors would like to thank Mr. Andrew Pouring of Yale University for the informative discussions on the kinetics of condensation and evaporation.

Drag Force (f_{p_i}) We have indicated (see Eq. 6) that the drag force on a particle depends on the velocity difference. In terms of a drag coefficient, C_{D_i} , the force on a single droplet in the condensed phase is given by:

$$\frac{f_{p_i}}{N_{p_i}} = \frac{f_{g p_i}}{N_{p_i}} = \frac{f_{p_i}}{N_{p_i}} = \frac{C_{D_i} \bar{A}_i \rho_g}{2} (V_g - V_{p_i}) |V_g - V_{p_i}| \quad 37a$$

This description assumes that all particles associated with the local number concentration, N_{p_i} , have the same average size. This restriction may be removed by introducing an appropriate size distribution law (Ref. 9). A $C_{D_i} \bar{A}_i$ would then be determined for each size group within the local number concentration. Equation 37a may be rewritten to provide the total force per unit volume of mixture and is given by:

$$f_{p_i} = \frac{\rho_{p_i}}{m_{p_i}} C_{D_i} \bar{A}_i \frac{\rho_g}{2} (V_g - V_{p_i}) |V_g - V_{p_i}| \quad 37b$$

In application, we shall assume that the droplets are spherical in shape so that Eq. 37b may be written:

$$f_{p_i} = \frac{3}{8} \rho_{p_i} \frac{C_{D_i} \rho_g}{8 \lambda_i r_{p_i}} (V_g - V_{p_i}) |V_g - V_{p_i}| \quad 37c$$

If the flow is in the Stokes regime then:

$$C_{D_i} = \frac{24}{Re_i} = \frac{12 \mu_g}{\rho_g r_{p_i} |V_g - V_{p_i}|} \quad 38$$

and we get:

$$\underline{f}_{pi} = \frac{9}{2} \frac{\rho_{pi} \mu_g}{8 \lambda_i r_{pi}^2} (V_g - V_{pi}) \quad 39$$

Thus, Eq. 39 or, in general, Eq. 37c may be used to account for the drag force between the gas phase and condensed phase.

Heat Transfer(\dot{Q}_{pi}) : The heat transfer between the gas phase and condensed phase depends on the temperature difference and can be expressed in terms of Newton's Law of Cooling. In terms a heat transfer coefficient, this is given by:

$$\frac{\dot{Q}(\sum V_j) P_i}{N_{pi}} = \frac{\dot{Q}_{pi}}{N_{pi}} = \lambda_i A_i (T_g - T_{pi}) \quad 40a$$

Thus, the heat transferred per unit volume of mixture to the i^{th} condensed species is given by:

$$\dot{Q}_{pi} = \frac{\rho_{pi}}{m_{pi}} \lambda_i A_i (T_g - T_{pi}) \quad 40b$$

and for spherical particles we get:

$$\dot{Q}_{pi} = \frac{3 \rho_{pi} \lambda_i}{8 \lambda_i r_{pi}} (T_g - T_{pi}) \quad 40c$$

The coefficient λ_i is dependent on the rate of evaporation, \dot{W}_{vi} , in virtue of the fact that this diffusing vapor is heated in flowing away from the droplet. The following development for λ_i is based on the work in Ref's 10 and 11.

We assume that the heat and mass transfer from the droplet is a quasi-steady process. The conduction term is modified by a correction factor, C_H , to account for convective heat transfer. Thus, the heat transferred to a single droplet in the i^{th} condensed phase is given by:

$$\frac{\dot{Q}_{pi}}{N_{pi}} = 4\pi r^2 k_i C_{Hi} \frac{dT}{dr} - (\dot{W}_{vi}^F) C_{pi} (T - T_{pi}) \quad 41$$

In virtue of the quasi-steady assumption, Eq. 41 may be integrated from $r = r_p$ to $r = \infty$ to give:

$$\frac{\dot{Q}_{pi}}{N_{pi}} = 4\pi k_i C_{Hi} r_{pi} (T_g - T_{pi}) \left\{ \frac{\frac{(\dot{W}_{vi}^F) C_{pi}}{r_{pi} 4\pi k_i C_{Hi}}}{e^{\frac{(\dot{W}_{vi}^F) C_{pi}}{r_{pi} 4\pi k_i C_{Hi}}} - 1} \right\} \quad 42$$

Now, we note that as $\dot{W}_{vi}^F \rightarrow 0$ the term in the brackets approaches unity, i.e.

$$\lim_{\dot{W}_{vi}^F \rightarrow 0} \left\{ \right\} \rightarrow 1 \quad 43$$

and we get:

$$\frac{\dot{Q}_{pi}}{N_{pi}} = 4\pi k_i C_{Hi} r_{pi} (T_g - T_{pi}) \quad 44$$

The usual definition of the film coefficient is given by:

$$\frac{\dot{Q}_{p_i}}{N_{p_i}} = h_{H_i} 4\pi r_{p_i}^2 (T_g - T_{p_i}) \quad 45$$

so that by comparison we get:

$$C_H = \frac{h_{H_i} r_{p_i}}{k_i} = \frac{1}{2} (Nu)_H \quad 46$$

Therefore, returning to Eq. 42, we may write:

$$\frac{\dot{Q}_{p_i}}{N_{p_i}} = 4\pi r_{p_i}^2 h_{H_i} (T_g - T_{p_i}) \left\{ \frac{\frac{(\dot{W}_{v,i}^F) C_{p_i}}{4\pi r_{p_i}^2 h_{H_i}}}{e^{\frac{(\dot{W}_{v,i}^F) C_{p_i}}{4\pi r_{p_i}^2 h_{H_i}}} - 1} \right\} \quad 47$$

or,

$$\dot{Q}_{p_i} = \frac{3\delta_{p_i}}{\delta_{L_i} r_{p_i}} h_{H_i} (T_g - T_{p_i}) \left\{ \right\} \quad 48$$

so that by Eq. 40c, we have:

$$\lambda_i = h_{H_i} \left\{ \frac{\frac{(\dot{W}_{v,i}^F) C_{p_i}}{4\pi r_{p_i}^2 h_{H_i}}}{e^{\frac{(\dot{W}_{v,i}^F) C_{p_i}}{4\pi r_{p_i}^2 h_{H_i}}} - 1} \right\} \quad 49$$

Correlations exist for h_{H_i} for evaporating droplets. Ref. 10 gives:

$$(Nu)_H = \frac{2 h_{H_i} r_{p_i}}{k_i} = 2 + 0.6 (Pr_i)^{1/3} (Re)^{1/2}$$

50

Equation 50 can be considered the best available correlation under a specified range of conditions. For example, Eq. 50 correlates the Nusselt No. with the Prandtl and Reynolds No's. for the following range of conditions:

$$0 < Re < 200$$

$80^\circ F < T_g < 400^\circ F$, for droplets of water, and various hydrocarbons evaporating into air. Therefore, the application of Eq. 50 to the severe conditions which may exist in the present problem must be performed with reservation. It will be assumed that in any case, the basic features of the flow field are retained when correlations of this kind are applied.

Mass Transfer: The analogy between the transfer of heat and mass permits us to express the evaporation rate in manner which parallels the development for the heat transfer. Thus, we define a film coefficient for mass transfer, h_{D_i} , such that:

$$\frac{\dot{W}_{vi}}{N_{vi}} = h_{D_i} A_i (P_{viT_p} - P_{vi})$$

51

In virtue of the similarity between heat and mass transfer when they occur in separate flow fields, we may expect a correlation for h_{D_1} similar to that for h_{H_1} . Ref. 10 gives:

$$(Nu)_M = \frac{2h_{D_1}r_{D_1}}{D_1} = 2 + 0.6(Sc_i)^{1/3}(Re_i)^{1/2} \quad 52$$

where the Schmidt No. replaces the Prandtl No. in Eq. 50 for the heat transfer coefficient.

It should be noted that Eq. 51 cannot predict the onset of condensation. The onset of condensation, or nucleation depends on the presence of (1) foreign impurities which may be in the form of previously condensed substances and (2) clusters of molecules formed of the species under consideration. When only nuclei of the second kind are present the situation is referred to as self-nucleation. In either case, there is a critical nucleus size required above which the droplet continues to grow. Approximate microscopic analysis for critical droplet size and for subsequent droplet growth are given in Ref. 5 and 12. These relations depend on knowledge of surface tension (or surface free energy in the case of solids) for which little is known particularly at the low temperatures of present interest. We will purposely delay specific analysis relating to nucleation and non-equilibrium condensation on the grounds that the mixing process of present interest will probably tend to be in thermodynamic equilibrium. The basis for this assumption rests on the fact the mixing region is boundary layer like and therefore is not subjected to strong streamwise temperature gradients.

The departure from phase equilibrium in supersonic and hypersonic wind tunnels depends on the existence of severe streamwise temperature gradients (Ref. 8). A discussion of multicomponent phase equilibrium is given in section IV.

Viscous Stress: In virtue of assumption (4) the transport of mass, momentum and energy due to random motion is limited to the gas phase. The pressure tensor is given by:

$$\underline{\pi} = -p_g \underline{\delta} + \underline{\tau}_g \quad 53$$

where, $\underline{\tau}_g \equiv$ viscous stress tensor

we take the usual Newtonian description for $\underline{\tau}_g$ given by:

$$\underline{\tau}_g = 2\mu_g \left[\frac{1}{2}(\nabla^* \underline{V}_g + \nabla \underline{V}_g) \right] - \frac{2}{3} \mu_g \nabla \cdot \underline{V}_g \underline{\delta} \quad 54$$

where μ_g is the absolute viscosity of the gas phase mixture and can be represented in terms of the gas concentrations of each of the species by (Ref. 13)

$$\mu_g = \sum_i \frac{\mu_i}{1 + \frac{w_i}{w_g} \sum_{j \neq i} \frac{w_g}{w_j} Y_j \Phi_{ij}} \quad 55$$

where,

$$\Phi_{ij} = \frac{\left[1 + \left(\frac{\mu_i}{\mu_j} \right)^{1/2} \left(\frac{W_j}{W_i} \right)^{1/4} \right]^2}{\frac{4}{\sqrt{2}} \left[1 + \frac{W_i}{W_j} \right]^{1/2}} \quad 56$$

and

$$\mu_i = A_i' (T_g)^{\omega_i} \quad 57$$

Heat Conduction: Thermal conductivity, as in the case of viscosity, derives from the random motion of the gas phase. Assuming Fourier's Law, we have:

$$\underline{q}_g = -k_g \nabla T_g \quad 58$$

where k_g is the thermal conductivity of the gas phase mixture.

Diffusion: Here, as in the description of viscosity and thermal conductivity, diffusion occurs only in the gas-phase. We assume Fick's Law for the diffusion of the gaseous species which is given by:

$$\underline{j}_{vi} = -\rho_g D_{ij} \nabla Y_{vi} \quad 59$$

where D_{ij} is the binary diffusion coefficient. In general, calculations will be made for specified Prandtl and Lewis No.'s so that there is no present need for

explicit relations for K_g and D_{ij} .

Relations 37c, 48, 51, 54, 58 and 59 complete the description of the rate processes. We have, for the moment, omitted a specific discussion of finite rate chemistry in order to focus our attention on the two-phase problem. The inclusion of chemical reactions requires statements for the \dot{W}_{vi}^c 's (Ref. 14).

We have mentioned under our discussion of evaporation rates that phase equilibrium may play an important role in the mixing process. It is, therefore, instructive to consider the relations which are applicable in the limiting case of multicomponent phase equilibrium.

IV. MULTICOMPONENT PHASE EQUILIBRIUM:

Classical developments on multicomponent phase equilibrium may be found in Ref's. 15, 16 and 17. We shall limit the present discussion to ideal mixtures for which the activity coefficients are identically equal to unity. Further, we shall assume the fugacities are equal to the pressures. The non-ideality of mixtures as expressed thru the activity coefficients and fugacities must be determined by means external to classical thermodynamics. These quantities are determined, in general, by experimental means. There appear to be no available results for the conditions of present interest. It should be noted, however, that the approximation regarding the fugacities is quite reasonable by virtue of the low pressures under consideration.

Thus, for the ideal mixture composed of perfect gases and condensed phases we define a vaporization equilibrium constant given by:

$$K_{fi} = \frac{\bar{Y}_i}{\bar{X}_i} \quad 60$$

where the bar indicates mole fraction. The vaporization equilibrium constant, K_{fi} , is a function of the mixture temperature for given total pressure, i.e.

$$K_{fi} = \frac{P_{si}}{P} \quad 61$$

where,

$$\log P_{si} = a_i + \frac{b_i}{T}$$

$$\sum_i \bar{Y}_i = 1$$

$$\sum_i \bar{X}_i = 1$$

The total molar concentration of a given species is defined by:

$$\bar{\beta}_i = \frac{\bar{Y}_i \bar{P}_g + \bar{X}_i \bar{P}_p}{\bar{P}_m} \quad 63$$

where $\bar{P}_m = \bar{P}_g + \bar{P}_p$ and the bar indicates a molar density, where,

$$\bar{P}_g = \sum_i \bar{P}_{vi} \quad 64$$

and

$$\bar{P}_p = \sum_i \bar{P}_{pi}$$

The degree of vaporization for the mixture is given by:

$$Z = \frac{\bar{P}_g}{\bar{P}_m} \quad 65$$

so that Eq. 63 may be written:

$$\bar{\beta}_i = \bar{Y}_i Z + \bar{X}_i (1-Z) \quad 66$$

or with the aid of Eq. 60;

$$\bar{\beta}_i = \bar{Y}_i Z + \frac{\bar{Y}_i}{K_{fi}} (1-Z) \quad 67a$$

$$= \bar{X}_i K_{fi} Z + \bar{X}_i (1-Z) \quad 67b$$

Thus, Eq. 67a gives:

$$\bar{Y}_i = \frac{\bar{\beta}_i K_{fi}}{1 + \sum (K_{fi} - 1)} \quad 68a$$

and Eq. 67b gives:

$$\bar{X}_i = \frac{\bar{\beta}_i}{1 + \sum (K_{fi} - 1)} \quad 68b$$

with the aid of Eq's. 62, Eq. 68a and b may be combined to give:

$$\sum_i \frac{\bar{\beta}_i}{\frac{1}{K_{fi} - 1} + \sum} \quad 69$$

Thus, if the total concentration ($\bar{\beta}_i$) of each species and the mixture temperature are known the concentration distribution of each species is determined. The degree of vaporization is obtained thru Eq. 69 and the gas-phase and condensed-phase concentrations are obtained thru Eq. 68a and b, respectively. For purposes of reference we have the additional relations for the total molar concentrations:

$$\bar{\beta}_i = \bar{\beta}_{ip} + \bar{\beta}_{ig} \quad 70$$

where

$$\bar{\beta}_{ip} = (1 - \bar{z}) \bar{x}_i \quad 71a$$

and

$$\bar{\beta}_{ig} = \bar{z} \bar{y}_i \quad 71b$$

In terms of total mass fractions, we have:

$$W_m = \frac{1}{\sum_i \frac{\beta_i}{W_i}} \quad 72$$

where,

$$\bar{\beta}_i = \beta_i \frac{W_m}{W_i} \quad 73$$

This analysis implies that each droplet in the condensed phase is a mixture of all condensing species. This would also be true in the case of non-equilibrium condensation or evaporation. Thus, as previously mentioned in the development of the conservation equations for the individual condensed species, the interpretation of these equations must be consistent with the manner in which condensation and evaporation is considered to take place. If each species i is considered to condense into droplets of species i is then the representation of the conservation equations for the individual species requires no interpretation. If, on the other hand, condensation and evaporation occur in accordance with the above equilibrium case, then there will exist only one kind of droplet composed

of all i condensing or evaporation species. In this case, the $3i$ condensed phase conservations are replaced by 3 condensed phase equations for mass, momentum and energy. There will be a single droplet velocity and temperature. The properties of the condensed phase will be given by:

$$\rho_p = \sum_i \rho_{pi} \quad 74$$

$$(C_p)_p = \frac{1}{\rho_p} \sum_i (C_p)_i \rho_{pi} \quad 75$$

The evaporation rate for the condensed phase will be given by:

$$\dot{W}_v = \sum_i \dot{W}_{vi} \quad 76$$

where

$$\dot{W}_{vi} = X_i \dot{W}_v \quad 77$$

Eq. 77 is required for the gas-phase species conservation equations. The droplet drag force and heat convection are also represented by single relations. Specific details of this discussion depend on the particular assumptions made with each case under consideration. This point is discussed in the following application.

V. APPLICATION TO CHEMICALLY FROZEN AXISYMMETRIC JET IN PHASE EQUILIBRIUM

In order to establish limits regarding the presence of a condensed phase we consider the flow to be in equilibrium. The existence of temperature and velocity equilibrium is an assumption based on the condition that the condensed phase is in the form of a cloud of small droplets. If the droplets are small then the heat convection and drag force are large and the resulting temperature and velocity lags will be small. Thus, the presence of small particles is an inherent condition in the equilibrium assumption. Surface tension effects are also neglected. The surface tension plays the governing role in determining the degree of supersaturation which occurs prior to condensation. This effect is primarily limited to the nucleation process where the nucleus size is of molecular dimensions (ref. 12). This effect on the non-equilibrium condensation decreases exponentially with the inverse of the droplet radius. In the absence of severe streamwise velocity and temperature gradients which is characteristic of the present mixing process, the assumption regarding equilibrium condensation of air appears to be a reasonable first approximation for the major portion of the flow field.

The phase equilibrium of hydrogen requires that the condensed fraction flash to vapor on entering the atmosphere. This equilibrium requirement is perhaps the limiting assumption in the present example particularly at the higher condensed phase concentrations (up to .45 in present calculations).

In any case, effects of the above assumptions on the flow field decrease as the mass fraction of condensed phase decreases. Thus, we consider the present calculation as a guide to the more complex physical phenomena actually

occurring and interpret the results as quantitatively accurate for small mass fraction of condensed phase, and qualitatively descriptive for other configurations.

Governing Equations :

In accordance with the above discussion, the governing equations 27 thru 33 reduce to the following system for the axisymmetric jet Fig. 1 with gas phase Prandtl and Lewis No.'s all equal to unity. These equations are taken to be identical in form for both laminar and turbulent flow with mean turbulent quantities replacing their laminar counterparts .

Continuity:

Global:

$$\frac{\partial \rho_m u r}{\partial x} + \frac{\partial \rho_m v r}{\partial r} = 0 \quad 78$$

Species:

$$\rho_m u \frac{\partial \beta_i}{\partial x} + \rho_m v \frac{\partial \beta_i}{\partial r} = \frac{1}{r} \frac{\partial}{\partial r} r k \frac{\partial \beta_i}{\partial r} \quad 79$$

Momentum:

$$\rho_m u \frac{\partial u}{\partial x} + \rho_m v \frac{\partial u}{\partial r} = \frac{1}{r} \frac{\partial}{\partial r} r k \frac{\partial u}{\partial r} \quad 80$$

Energy:

$$\rho_m u \frac{\partial H_m}{\partial x} + \rho_m v \frac{\partial H_m}{\partial r} = \frac{1}{r} \frac{\partial}{\partial r} r k \frac{\partial H_m}{\partial r} \quad 81$$

The appropriate boundary and initial conditions for a jet of radius a are:

for $x = 0$, $0 \leq r < a$

$$u = u_j , v = 0 , H_m = H_j , \beta_{O_2} = \beta_{N_2} = 0$$

$$\beta_{H_2} = 1$$

for

$$x = 0 , r \geq 0$$

$$u = u_e , v = 0 , H_m = H_e , \beta_{O_2} = \beta_{O_2e} , \beta_{N_2} = \beta_{N_2e} , \beta_{H_2} = 0$$

$$x \geq 0$$

$$\lim_{r \rightarrow \infty} H = H_e , u = u_e , v = 0 , \beta_{O_2} = \beta_{O_2e} , \beta_{N_2} = \beta_{N_2e} , \beta_{H_2} = 0$$

with the regularity condition applied along the jet centerline.

for laminar flow we have:

$$k = \mu g$$

and for turbulent flow we have:

$$k = (\epsilon \rho)_m$$

where ϵ is the eddy viscosity coefficient.

In virtue of the unity Prandtl and Lewis No.'s, similarity in the equations for β_i , u and H_m exists. Further, since the boundary conditions are similar the system admits Crocco relations for H_m and the β_i 's, i.e. H_m and β_i are linearly dependent on the velocity, u . Thus, the problem reduces to that of determining the solution for the velocity distribution. This together with equations of state and appropriate phase equilibrium relations fully determine

the problem.

The solution for u is more readily handled in a corresponding incompressible plane. Following Ref. 18 we introduce the following stream function:

$$\begin{aligned}\rho_m u r &= \rho_e u_e \psi \psi_r \\ -\rho_m v r &= \rho_e u_e \psi \psi_x\end{aligned}\tag{82}$$

Introducing Von Mises transformation, i.e. $x, r \rightarrow x, \Psi$ where,

$$r^2 = \int_0^\Psi \frac{2\rho_e u_e}{\rho_m u} \psi' d\psi'\tag{83}$$

and applying a modified Oseen approximation in form,

$$\frac{\mu_g \rho_m r^2 u}{\rho_e^2 u_e^2 \psi^2} \cong f(x)\tag{84}$$

where the additional transformation

$$\xi = \int_0^x \frac{f(x')}{\psi_j} dx'\tag{85}$$

is introduced, the momentum equation becomes:

$$\frac{\partial v}{\partial \xi} = \frac{\psi_j}{\psi} \frac{\partial}{\partial \psi} \left[\psi \frac{\partial v}{\partial \psi} \right]\tag{86}$$

where,

$$\psi_j = a \left(\frac{\rho_j u_j}{\rho_e u_e} \right)^{1/2} ; \quad U = \frac{u}{u_e} \quad 87$$

Following Libby (Ref. 14), for laminar flow the approximation function $f(x)$ is evaluated along the jet centerline yielding the inverse transformation:

$$\frac{x}{\psi_j} = \int_0^{\xi} \frac{\rho_e u_e}{(\mu g)_t} d\xi' \quad 88$$

For turbulent flow a model suitable under present conditions is:*

$$f(x)_t = \frac{n r_{1/2}}{u_e} (u_e - u_t) \quad 89$$

where $r_{1/2}$ is the "half radius" defined by:

$$(u)_{r_{1/2}} = \frac{1}{2} (u_e + u_t) \quad 90$$

and n is the Prandtl mixing length constant.

The inverse transformation then becomes:

$$\frac{x_t}{\psi_j} = \int_0^{\xi} \frac{1}{f(x)_t} d\xi' \quad 91$$

* Note: This model does not predict reasonable results under other conditions: For example, cases where $U_j = 1$. However, the modified eddy viscosity model applied in Ref. 4 is not suitable under present conditions.

The initial and boundary conditions on the momentum equation become:

$$\begin{aligned} V(0, \psi) &= V_j & ; & \quad 0 < \psi < \psi_j \\ &= 1 & ; & \quad \psi > \psi_j \end{aligned}$$

and

$$\lim_{\xi \rightarrow \infty} V(\xi, \psi) \rightarrow 1$$

With the regularity condition applied along the jet centerline, $\Psi = 0$.

The solution of the momentum equation is given by the offset circular probability function P;

$$P = \frac{1-V}{1-V_j} = \frac{\psi_j}{2\xi} e^{-\frac{(\psi/\psi_j)^2}{4\xi/\psi_j}} \int_0^1 e^{-\frac{\psi'^2}{4\xi/\psi_j}} I_0 \left[\psi' \left(\frac{\psi}{\psi_j} \right) \left(\frac{2\xi}{\psi_j} \right)^{-1} \right] \psi' d\psi' \quad 92$$

which has been tabulated in Ref. 19.

In order to perform the inverse transformations to the physical plane (Eq. 83 and 88 of 91), the thermodynamic properties must be determined. The stagnation enthalpy is given by:

$$H_m = \frac{H_e(V-V_j) + H_j(1-V)}{1-V_j} = \frac{u^2}{2} + h_m \quad 93$$

and the total species concentrations are given by:

$$\beta_{O_2} = \beta_{O_2e} \frac{U - U_j}{1 - U_j}$$

$$\beta_{N_2} = \beta_{N_2e} \frac{U - U_j}{1 - U_j}$$

$$\beta_{H_2} = \frac{1 - U}{1 - U_j}$$

94

The Equation of State is given by:

$$P = p_e = \sum \left\{ \frac{\beta_{O_2g}}{W_{O_2}} + \frac{\beta_{N_2g}}{W_{N_2}} + \frac{\beta_{H_2g}}{W_{H_2}} \right\} RT$$

95

where,

$$p_{O_2g} = \sum \frac{\beta_{O_2g}}{W_{O_2}} RT$$

$$p_{N_2g} = \sum \frac{\beta_{N_2g}}{W_{N_2}} RT$$

$$p_{H_2g} = \sum \frac{\beta_{H_2g}}{W_{H_2}} RT$$

96

The stagnation enthalpy is given by:

$$H_m = \frac{U^2}{2} + \beta_{O_2} \left\{ h_{O_2g} - \frac{\beta_{O_2} - \beta_{O_2g}}{\beta_{O_2}} L_{O_2} \right\}$$

$$+ \beta_{N_2} \left\{ h_{N_2g} - \frac{\beta_{N_2} - \beta_{N_2g}}{\beta_{N_2}} L_{N_2} \right\}$$

$$+ \beta_{H_2} \left\{ h_{H_2g} - \frac{\beta_{H_2} - \beta_{H_2g}}{\beta_{H_2}} L_{H_2} \right\}$$

97

where,

$$h_{ig} = h_{ig}(T) \quad 98$$

and

$$L_i = L_i(T) \quad 99$$

The equilibrium conditions used in the present calculation will be an approximation to the results presented in section IV. We shall consider the partial pressure of a species in two phases to be equal to the saturation pressure corresponding to the existing temperature. This is exact when only one of the species condensed. However, the error is small in virtue of the steep slope of the vapor-pressure curves. That is, the range of temperature over which two phases of each species exist in comparable proportions is extremely narrow. This, coupled with the close similarity between Oxygen and Nitrogen justifies the assumption.

Thus we have:

Nitrogen:

$$\log_{10} P_{N_2}(\text{mmHg}) \cong 7.6589 - \frac{359.093}{T(^{\circ}\text{K})} \quad 100$$

Oxygen:

$$\log_{10} P_{O_2}(\text{mmHg}) = 9.131 - \frac{482}{T(^{\circ}\text{K})} \quad 101$$

where, Eq. 100 is given in Ref. 20 and Eq. 101 is a curve fit of data given in Ref. 21.

Relations 94 thru 101 fully determine the nature of the flow field in the velocity plane and supply the required thermodynamic variables for the transformation to physical coordinates via Eq.'s 83, 88 or 91 and the viscosity relation, Eq. 55.

Method of Solution in the Velocity Plane

The solution in the velocity plane can be carried out for the following given data:

- (a) Altitude
- (b) Hydrogen tank conditions with an isentropic expansion to atmospheric conditions
- (c) Vehicle trajectory i.e. u_e vs Altitude

Now, for each velocity ratio $U_j < U < 1$ the computations proceed in the following manner:

- (1) Assume T
- (2) Assume O_2 and N_2 exist in two phases so that $P_{N_2}^g$ and $P_{O_2}^g$ are determined by Eq.'s 100 and 101 respectively.

- (3) P_{H_2} is determined by:

$$P_{H_2} = P_c - P_{N_2}^g - P_{O_2}^g$$

(4) $\beta_{O_2 g}$ and $\beta_{N_2 g}$ are determined by Eq.'s 93, i.e.:

$$\beta_{O_2 g} = \frac{P_{O_2 g}}{P_{H_2}} \frac{\beta_{H_2}}{W_{H_2}} W_{O_2}$$

and

$$\beta_{N_2 g} = \frac{P_{N_2 g}}{P_{H_2}} \frac{\beta_{H_2}}{W_{H_2}} W_{N_2}$$

(5) (a) if $\beta_{O_2 g} < \beta_{O_2}$ then assumption (2) for O_2 is valid.

Similarly for N_2 .

(b) if $\beta_{O_2 g} > \beta_{O_2}$ then assumption (2) is incorrect and we

take all O_2 in the gas phase. Similarly for N_2 .

(6) With (1) and the results of (4) and (5), the stagnation enthalpy must be checked. In Eq. 97 H_m and u are known and the β_i 's have just been determined. Thus, with (1) we can determine whether the stagnation enthalpy relation is satisfied. If it is not satisfied, a new temperature is assumed, step (1), and the computations are repeated. This procedure is carried out for each velocity ratio U in the range $U_j < U < 1$ corresponding to each set of given data. Calculations were carried out for the following given data:

Altitude (KM)	P_e ATM	T_e (°K)	u_e F. P. S.	H_e 61/gm	H_j Cal/gm	u_j F. P. S.
60	0.000252	254	7330	653	175	2785
40	0.00298	261	4990	340	175	2460
20	0.0545	216	2420	117	175	1880

Additional quantities which were taken as constants in the calculations are:

$$\beta_{O_2} = 0.232$$

$$\beta_{N_2} = 0.768$$

$$L_{O_2} \cong 65 \frac{\text{cal.}}{\text{gm}}$$

$$L_{N_2} \cong 57 \frac{\text{cal.}}{\text{gm}}$$

Hydrogen fuel tank:

$$T_t = 20.0^\circ\text{K sat.}$$

$$a = 1 \text{ inch}$$

Thermodynamic properties used in the calculations are given in Ref.'s 20 and 21.

VI. DISCUSSION

The description of the phenomena resulting from the dumping of cryogenic hydrogen into the atmosphere requires a departure from the usual one-dimensional pipe flow models found in the literature for treating two-phase flows. The class of problems of interest depend on mixing for their description and therefore require a multidimensional analysis. Since the present problem involves the mixing into air of cryogenic hydrogen with a normal boiling point substantially lower than the air we will, in general, encounter small condensed phase mass fractions. Thus, in such a mixing process, the condensed phase will form a dilute suspension in the gas phase. In the present work a model is developed for treating the flow of a dilute suspension of condensing and evaporating components. Velocity and temperature lags between the phases are accounted for in terms of appropriate momentum and energy interaction parameters. Evaporation and condensation is accounted for in terms of appropriate mass transfer and the associated momentum and energy transfer parameters. In addition to these inter-phase transfers we have gas phase viscosity, thermal conductivity, and diffusion of the gas phase components. The description of the inter-phase transport phenomena poses a substantial problem in itself. There is a general lack of fundamental constitutive relations to account for the simultaneous occurrence of the above discussed inter-phase rate processes. This is particularly true of the nucleation and condensation processes at the low temperatures of current interest. In any case, this area requires much additional work. Thus, it is necessary to adopt a semiempirical approach which in general will be qualitatively valid and in certain limiting cases will

provide quantitatively valid results.

In the present numerical example the boundary conditions are such that the flow will be chemically frozen. This removes the added complication of rate chemistry and permits this preliminary analysis to focus on multi-phase effects. In particular, the analysis and numerical results for a diffusion controlled axisymmetric jet are presented. Fig's. 1 thru 4j show the jet geometry and the distributions of the pertinent variables, respectively. Fig. 1 is a schematic representation of the axisymmetric jet showing the inner cone composed essentially of undisturbed two-phase hydrogen. In crossing the cone boundary, the hydrogen flashes to vapor in accordance with the equilibrium assumption. The remaining figures show the radial and axial distributions of mixture mass fractions of condensed phase and gas phase components. In addition, temperature and velocity distributions are presented. These results are for the altitudes of 20, 40 and 60 KM. There are some general features characteristic of all altitude determinations. We note that the air is completely condensed until certain radial and axial positions are attained. At these points there is a rapid spacewise transition from solid to vapor accompanied by a plateau or an actual decrease in temperature. The rapid phase change is due to the large rate of increase in saturation pressure with temperature. Thus, a point is reached where the local pressure and mixture concentrations cannot support the condensed phase. The energy required for the evaporation is derived from the gas phase and consequently inhibits a temperature increase in this transition zone. A feature of considerable interest is the streamwise extent within which two phases exist. The two limiting cases of laminar and fully

developed turbulent flows have been treated and provided the maximum and minimum "two-phase lengths", respectively. The long lengths in the laminar flow are attributed to the low viscosities associated with the low temperatures. The turbulent model used in the present case provides an eddy viscosity based strictly on dynamic quantities, i. e. on the velocity difference between the axis and free stream. This could account for the large $\sim 1000/1$ ratio for the laminar to turbulent two-phase lengths on the axis. We expect ratios of the order of $100/1$. In any case, the actual two-phase lengths depend on the degree to which turbulence has developed. Thus, we can only estimate that for the present problem two-phase lengths on the order of hundreds of feet can be expected.

Regarding effects on ignition and combustion of hydrogen we note that two-phase flow does not exist above $T \cong 50^\circ\text{K}$. At temperatures of this magnitude, we cannot expect any chemical activity. This implies that even for appropriate (high temperature) free stream conditions, the existence of two-phase flow provides an additional ignition time delay factor. That is, before ignition occurs re-evaporation must take place where temperature rises are inhibited. This is characteristic of ignition delay.

It has been pointed out that the equilibrium assumption applied to the hydrogen is perhaps the limiting assumption in the present jet problem. In order to assess this assumption a "partial equilibrium" analysis is currently being programmed for digital computation. In particular, two-phase hydrogen is injected into an air stream where it is assumed that the air condenses in

equilibrium. On the otherhand, the condensed hydrogen particles are allowed to evaporate according to an appropriate rate law. Included in this work will be the effects of small particle evaporation and condensation in rarefied atmospheres pertinent to the high altitude range of present interest. In order to provide an insight into the effect of finite rate evaporation the limiting case of zero interphase mass transfer is shown in Fig. 5 . The details of the partial equilibrium analysis will be available under separate cover at a later date.

REFERENCES

1. Taub, P.A., Slot Injection of Reactive Gases in Laminar Flow With Application to Hydrogen Dumping, GASL Technical Report No. 332, Jan. 1963.
2. Libby, P.A., Schetz, J.A., Approximate Analysis of Slot Injection of a Reactive Gas in Laminar Flow, GASL Technical Report No. 293, Nov. 1962.
3. Libby, P.A., Pergament, H.S., Taub, P., Engineering Estimates of Flow Lengths Associated With the Combustion of Hydrogen-Air Mixtures During a Launch Trajectory, GASL Technical Report No. 330, Dec. 1962.
4. Rosenbaum, H., Axisymmetric Laminar and Turbulent Jets of Hydrogen with Simple Chemistry, GASL Technical Report No. 331, Jan. 1963.
5. Wegener, P.P., and Mack, L.M., Condensation in Supersonic and Hypersonic Wind Tunnels, Advances in Applied Mechanics, Vol. 5, pp. 307-447, 1958.
6. Hirschfelder, Curtiss, and Bird, Molecular Theory of Gases and Liquids, John Wiley and Sons, 1954.
7. Edelman, R.B., The Flow of a Dilute Suspension of Solids in a Laminar Gas Boundary Layer, Doctoral Thesis, Yale University, 1962.
8. Pouring, A.A., An Experimental and Analytical Investigation of Homogeneous Condensation of Water Vapor in Rapid Expansions, Doctoral Thesis, Yale University, 1963 (in preparation)
9. Hermans, J.J., Flow Properties of Disperse Systems, North Holland Publishing Co., pp. 319-322, 1953.
10. Ranz, W.E., and Marshall, W.R. Jr., Evaporation from Drops, Chemical Engineering Progress, Part I, Vol. 48, No. 3, March 1952, pp. 141-146 and Part II, Vol. 48, No. 4, April 1952, pp. 173-180.

11. Graves, C.C. and Bahr, D.W., Basic Considerations in the Combustion of Hydrocarbon Fuels in Air, Chapter I, NACA, Report 1300, 1957.
12. Frenkel, J., Kinetic Theory of Liquids, Dover Publishing Co., Chapter 7, 1955.
13. Bromley, L.A. and Wilke, C.R., Viscosity Behavior of Gases, Industrial and Engineering Chemistry, Vol. 43, July 1951.
14. Libby, P.A., Theoretical Analysis of Turbulent Mixing of Reactive Gases with Application to Supersonic Combustion of Hydrogen, A.R.S. Journal, Vol. 32, No. 3, March 1962.
15. Guggenheim, E.A., Thermodynamics, North Holland Publishing Co., Chapter 5 and 7, 1957.
16. Hall, N.A. and Idele, W.E., Engineering Thermodynamics, Prentice-Hall Publishing Co., Chapter 12, 1960.
17. Zemansky, M.W., Heat and Thermodynamics, McGraw-Hill Publishing Co., Chapter 19, 1957.
18. Kleinstein, G., An Approximate Solution for the Axisymmetric Jet of a Laminar Compressible Fluid, Polytechnic Institute of Brooklyn, Sept. 1962.
19. Masters, J.I., Some Applications in Physics of the P. Function, Journal of Chemical Physics, Vol. 23, Oct. 1955.
20. Tables of Thermodynamic Properties of Gases, National Bureau of Standards, Circular 564, Nov. 1955.
21. Mullins, J.C., Ziegler, W.T., and Kirk, B.S., The Thermodynamic Properties of Oxygen From 20° to 100°K, Georgia Institute of Technology, TR-2 (N.B.S. MR-8), March 1, 1962

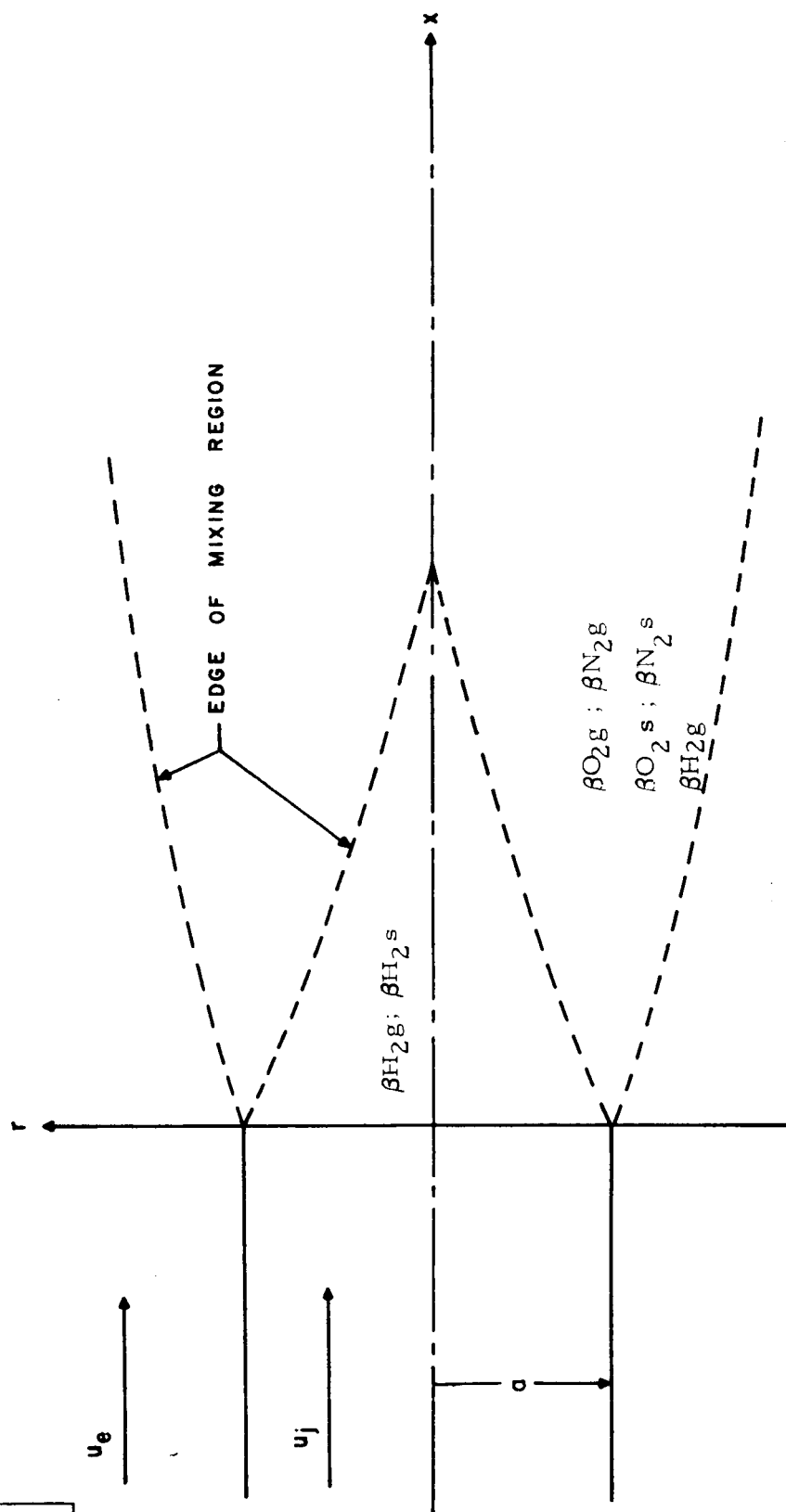


FIG. 1 SCHEMATIC OF FLOW REGION

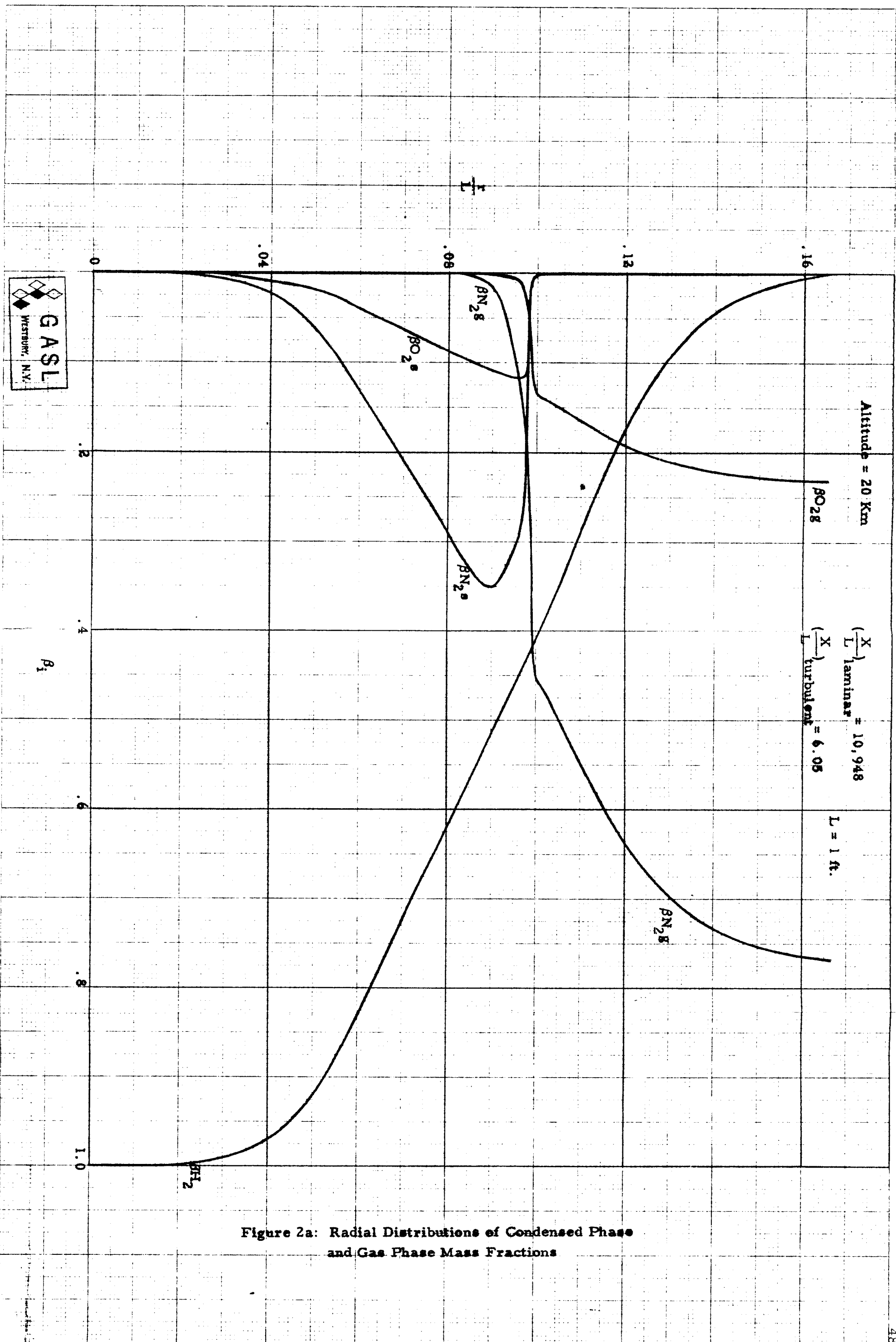


Figure 2a: Radial Distributions of Condensed Phase and Gas Phase Mass Fractions

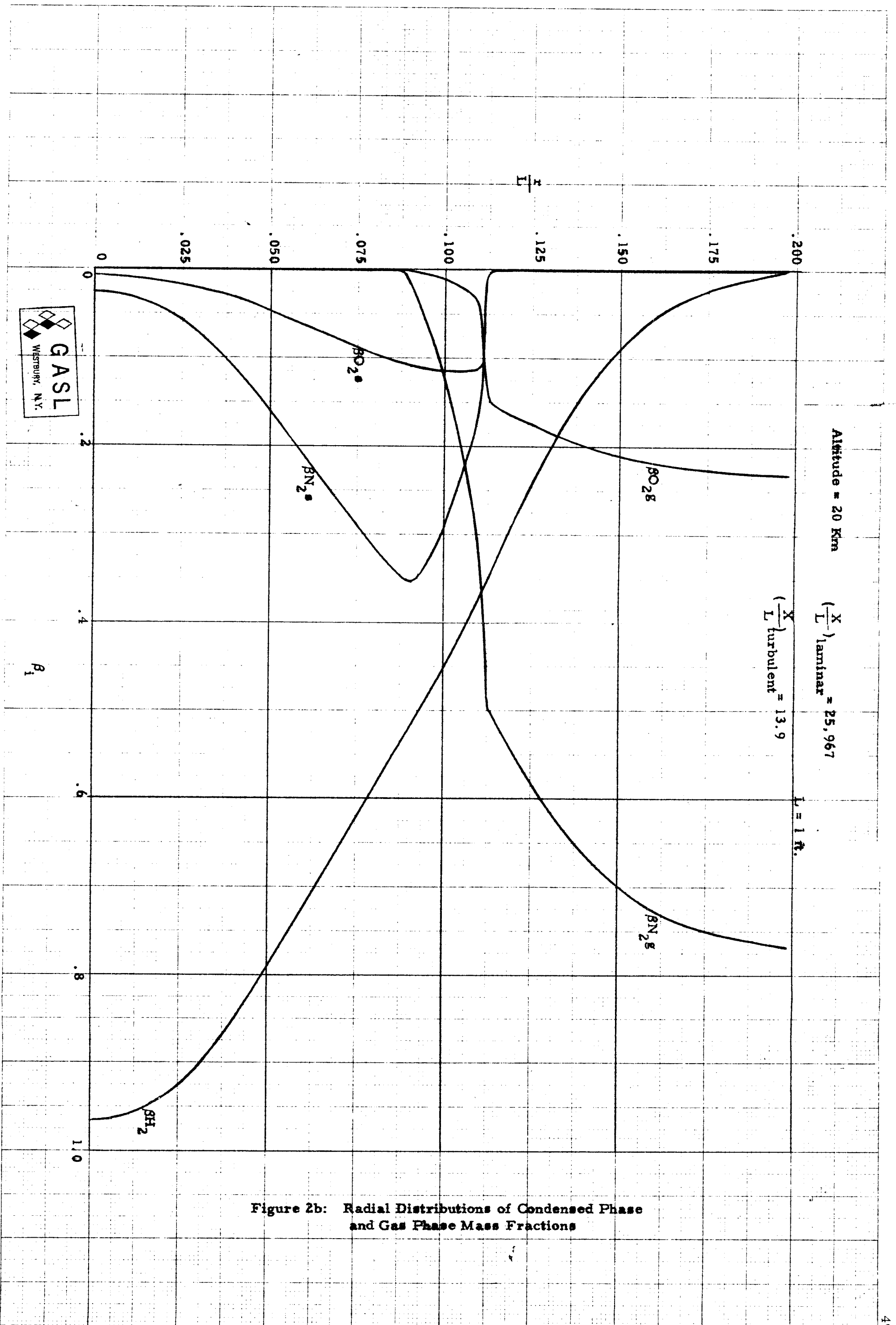


Figure 2b: Radial Distributions of Condensed Phase and Gas Phase Mass Fractions

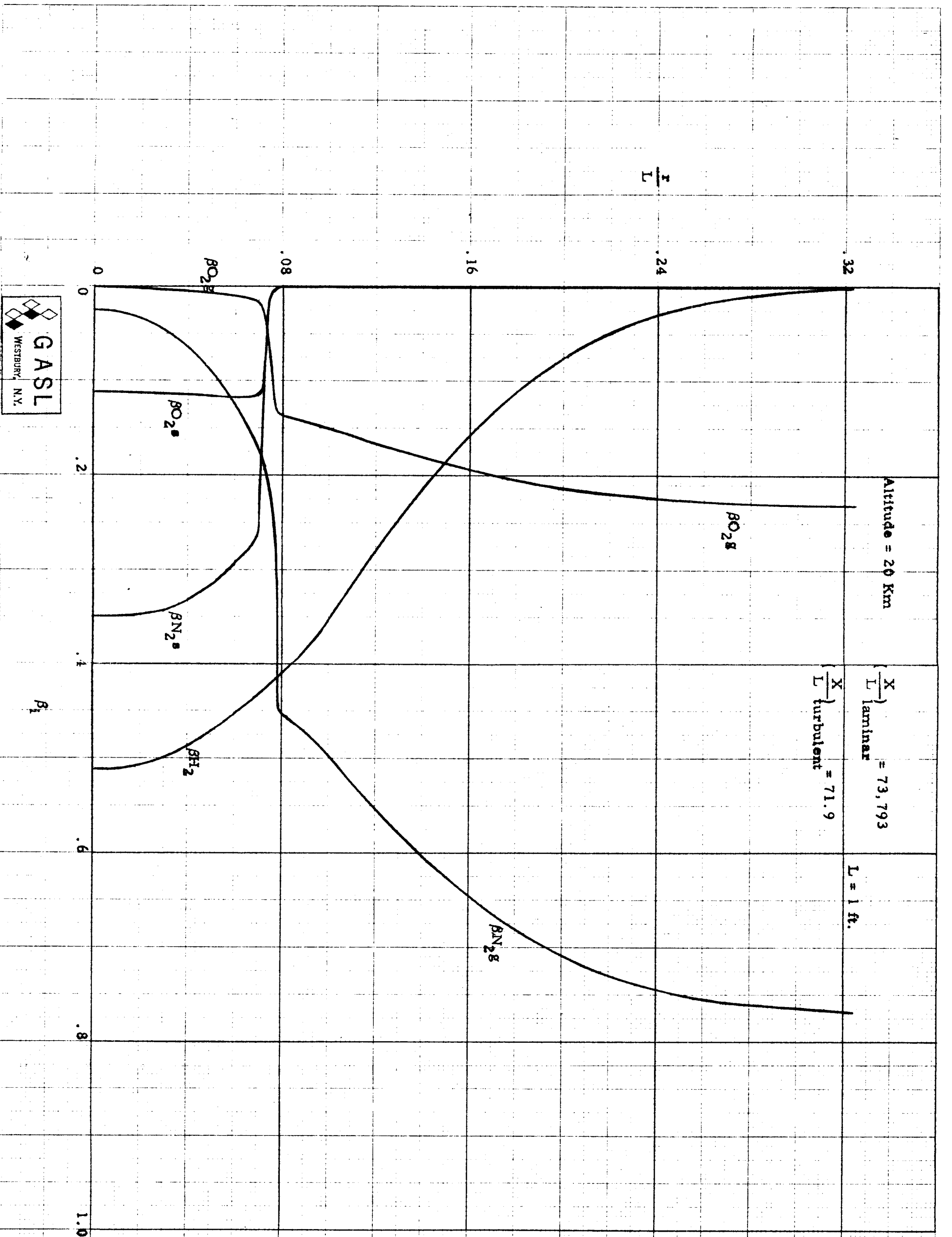


Figure 2c: Radial Distributions of Condensed Phase and Gas Phase Mass Fractions

Figure 2d: Radial Distributions of Velocity
and Temperature at 20 Km

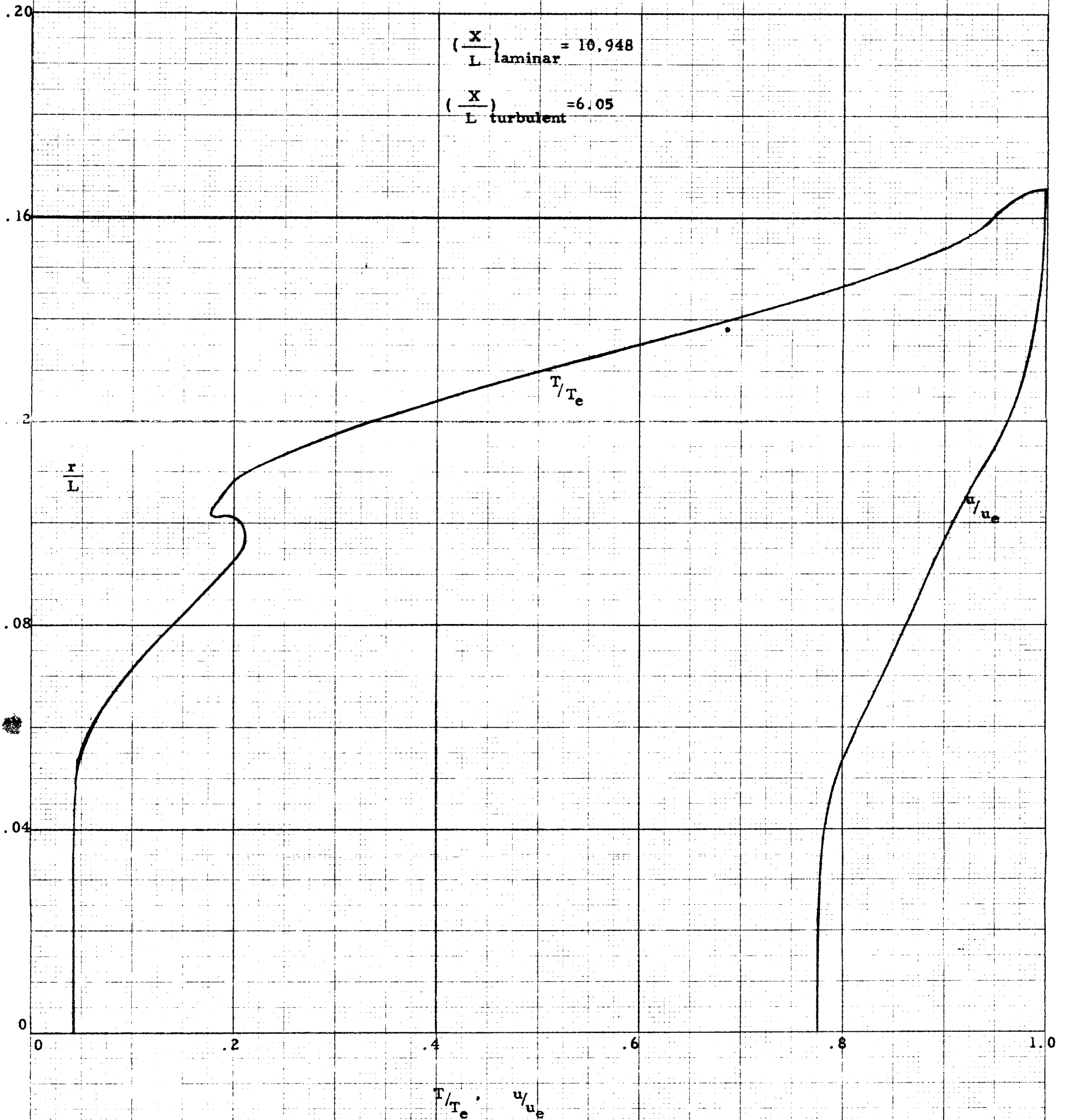


Figure 2e: Radial Distribution of Velocity
and Temperature at 20 Km

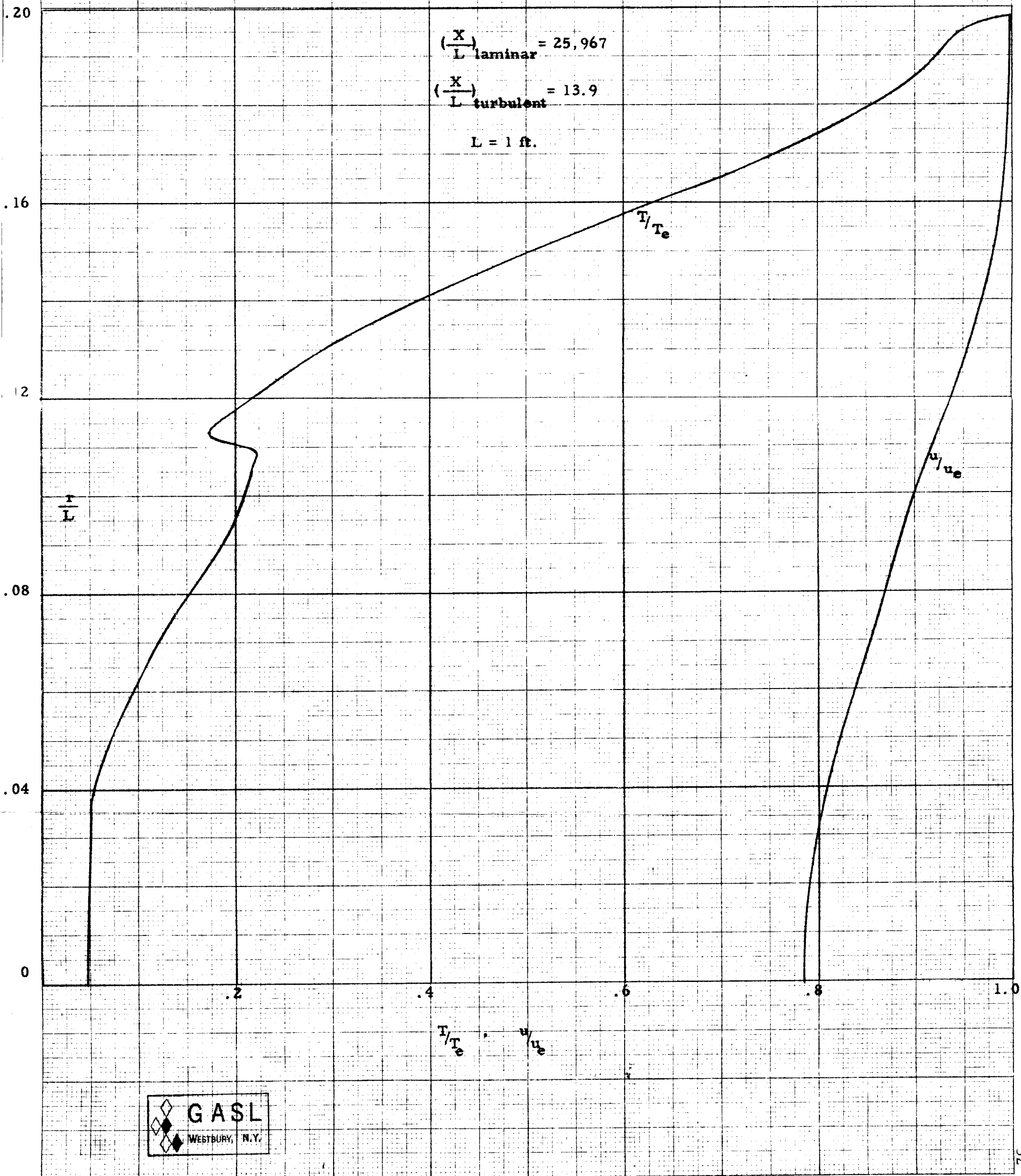


Figure 2f: Radial Distribution of Velocity
and Temperature at 20 Km

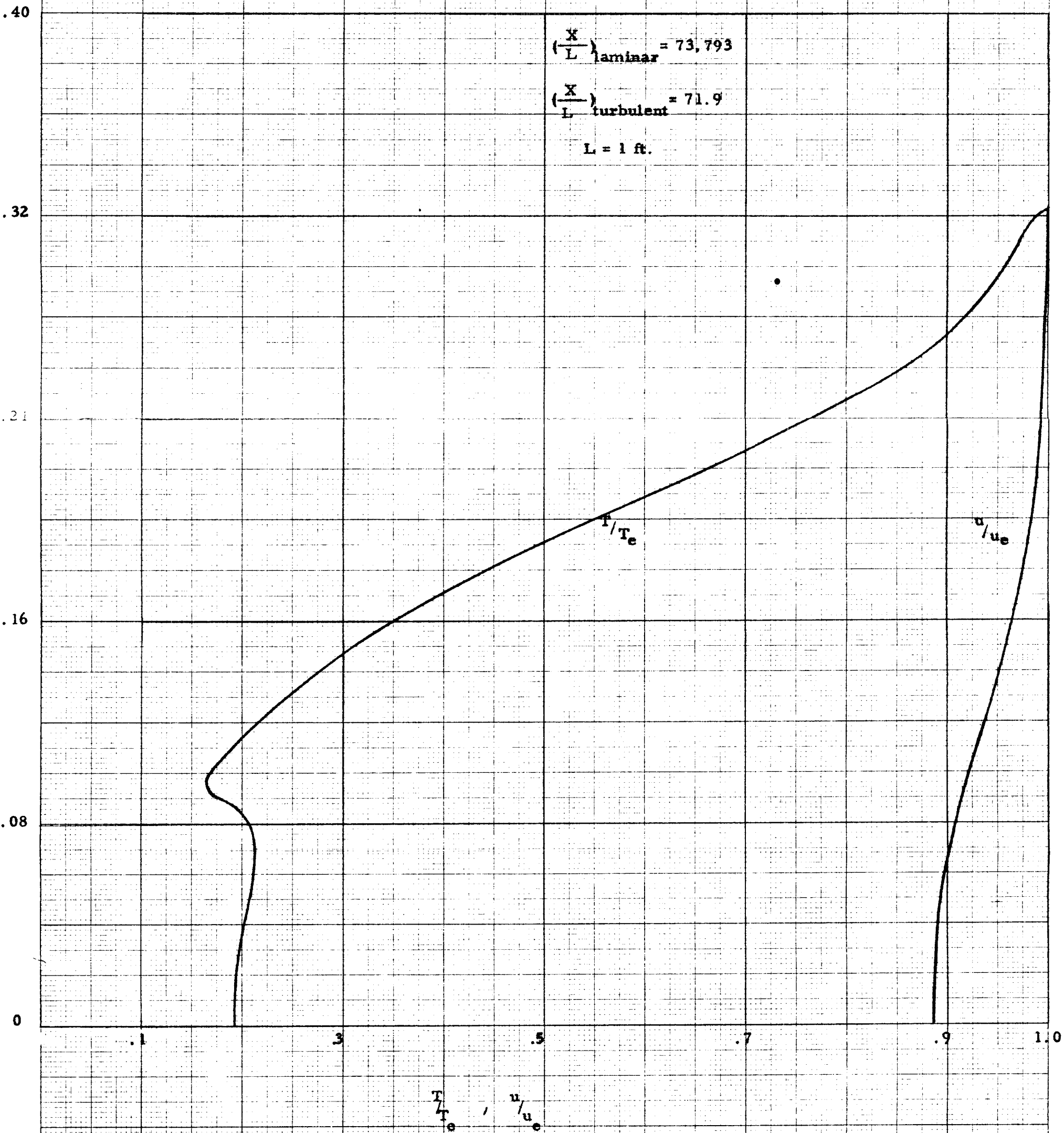
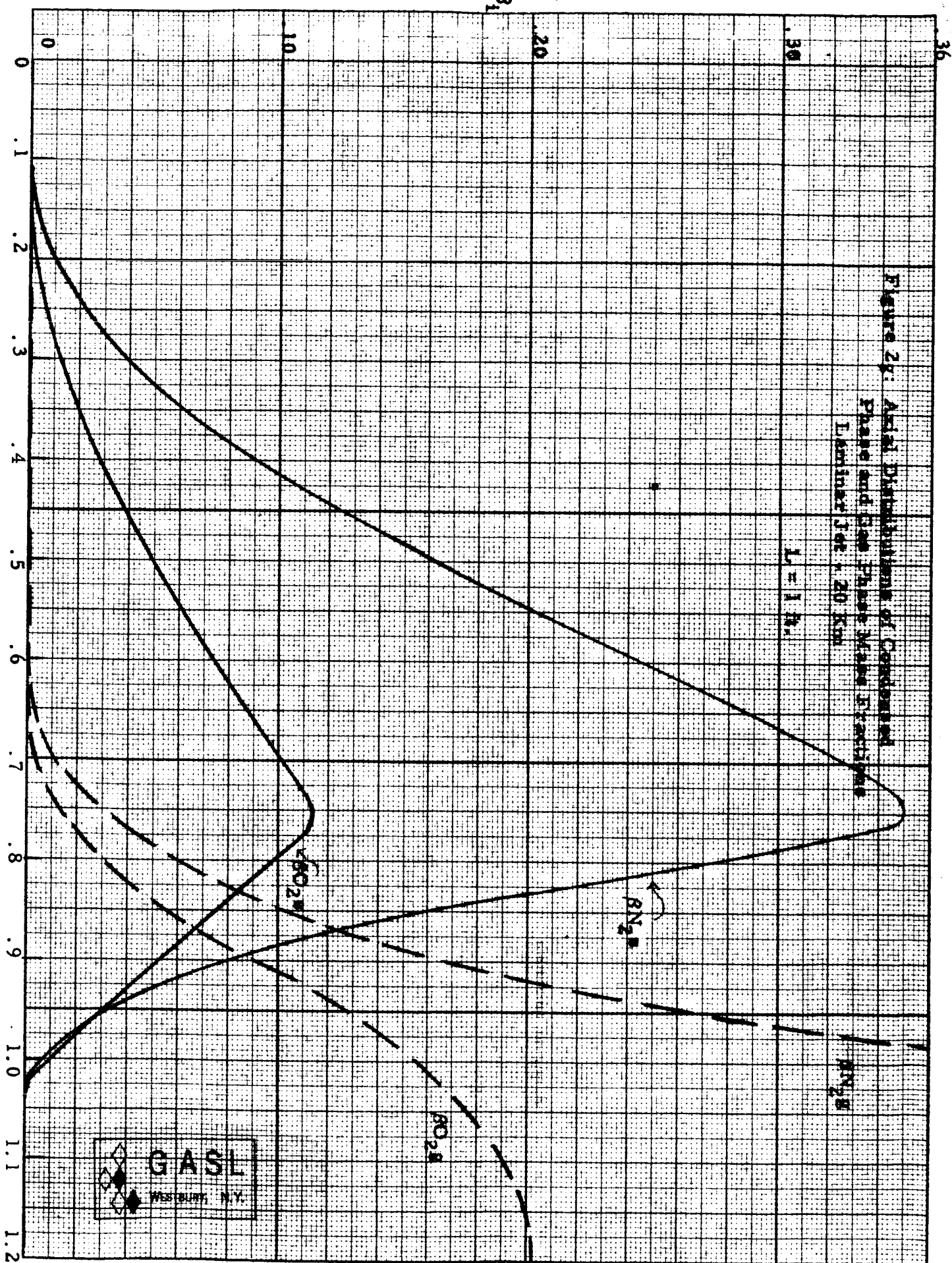


Figure 2g: Axial Distributions of Condensed
Phase and Gas Phase Molar Fractions
Laminar Jet, 20 km

$L = 1 \text{ ft.}$



GASL
WESTBURY, N.Y.

$(\frac{X}{L}) \times 10^{-5}$

EUGENE DIETZGEN CO.

ER
PRAP
DIETZ
MILLIMETER

246

Figure 2b. Axial Distributions of Velocity
and Temperature
Laminar Flow - Altitude = 20 Km
 $L_e = 1 \text{ M}$

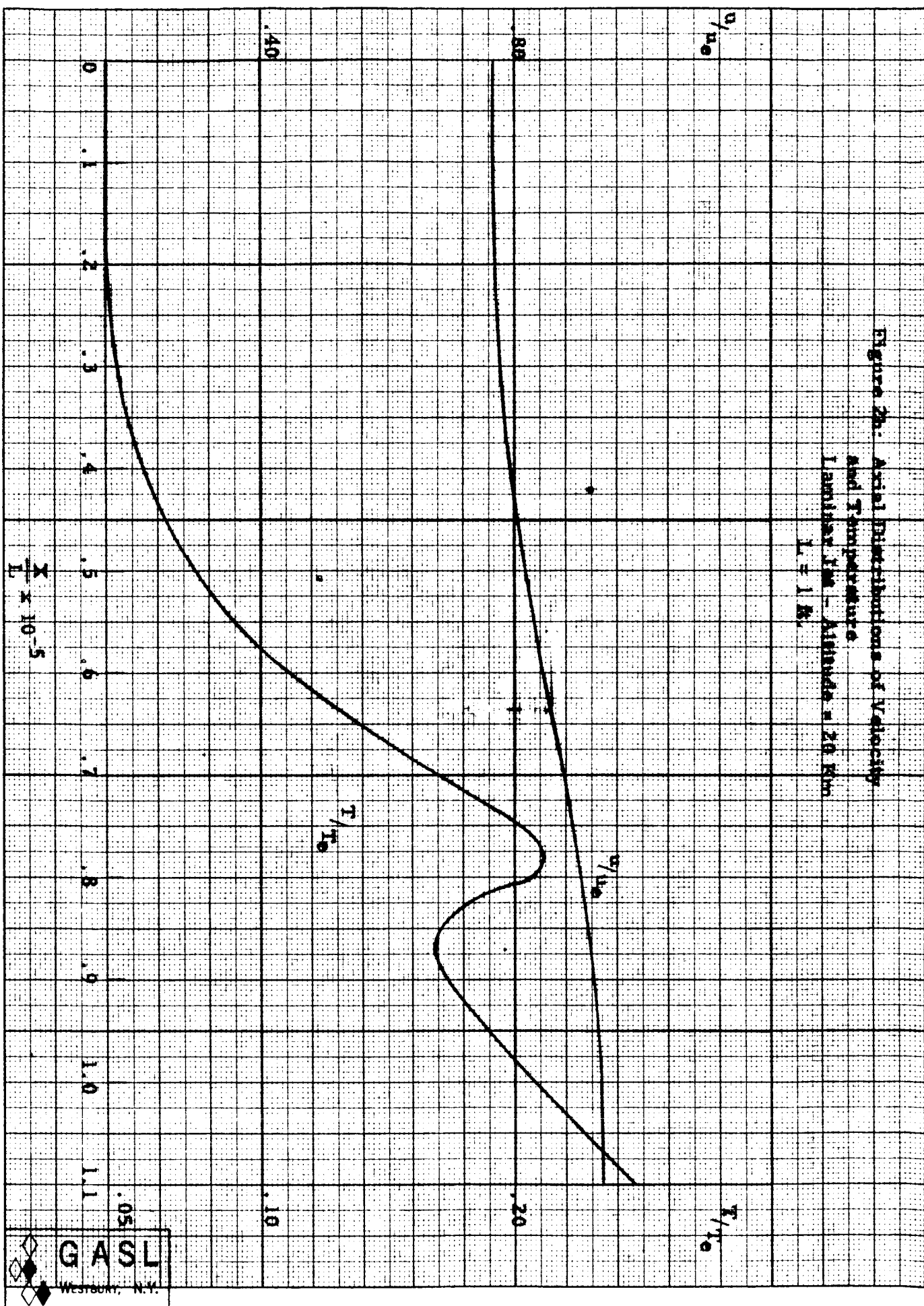
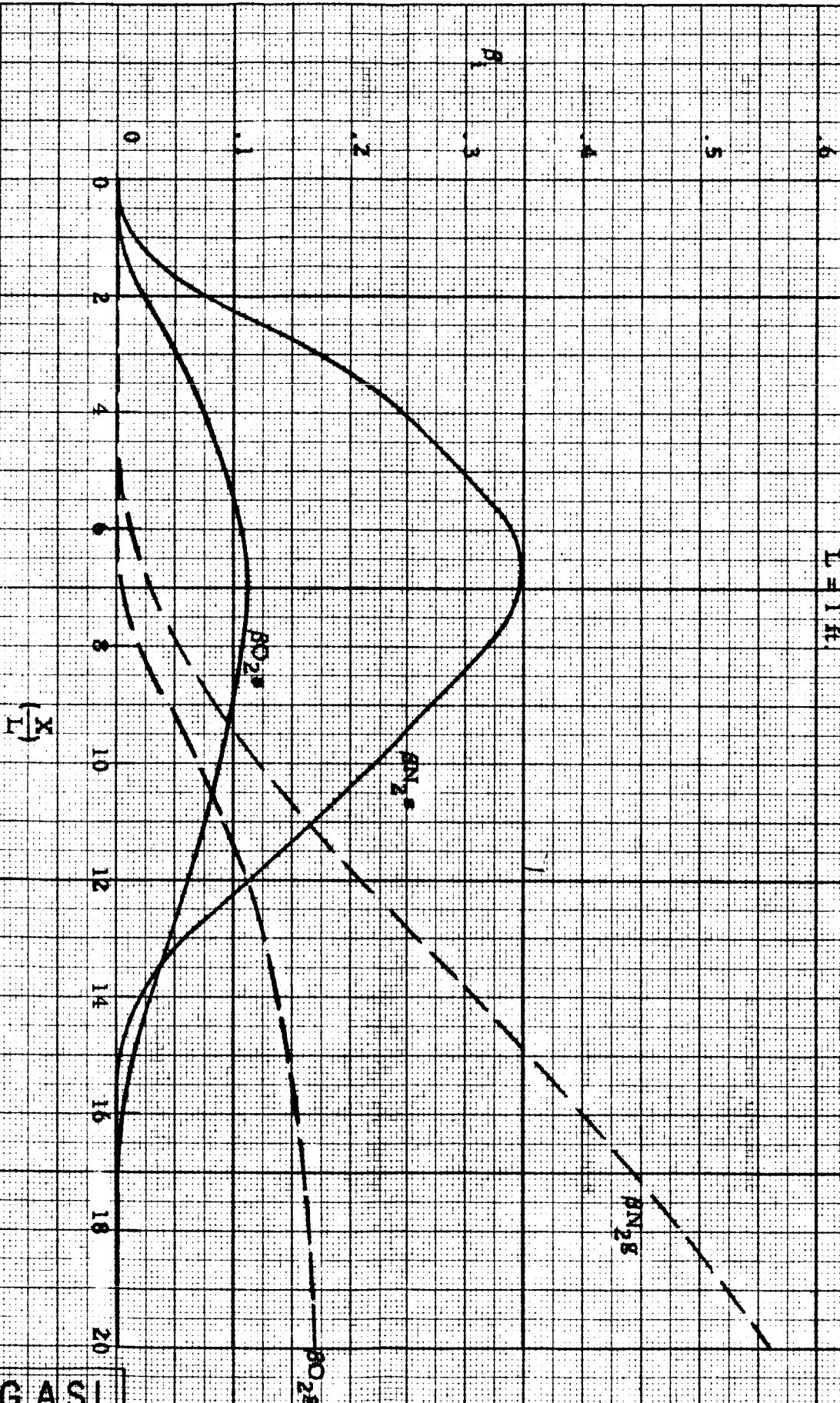


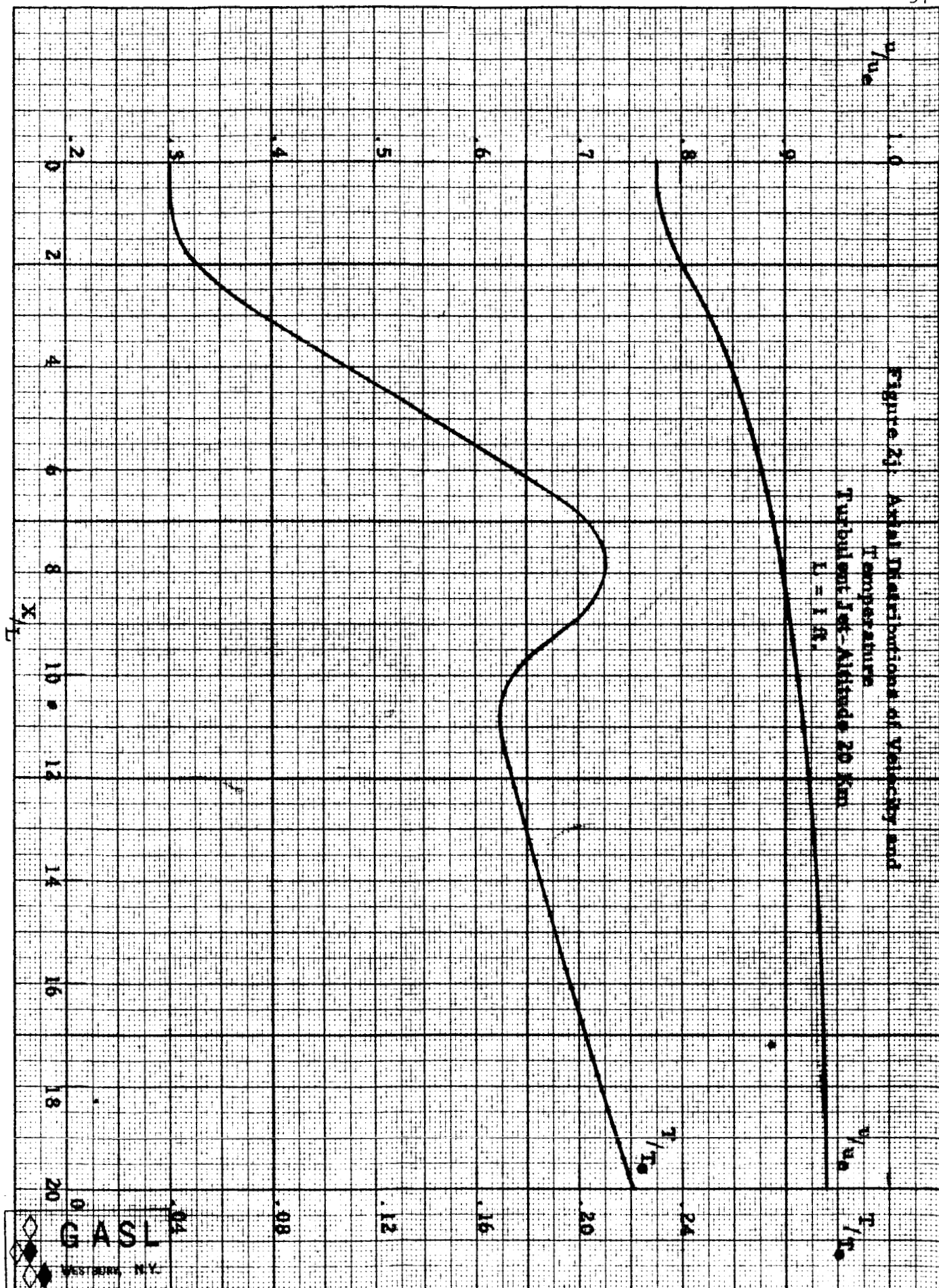
Figure 21: Axial Distributions of Condensed Phase

and Gas Phase Mass Fractions

Turbulent Jet - 20 Km

$L = 1$ ft.





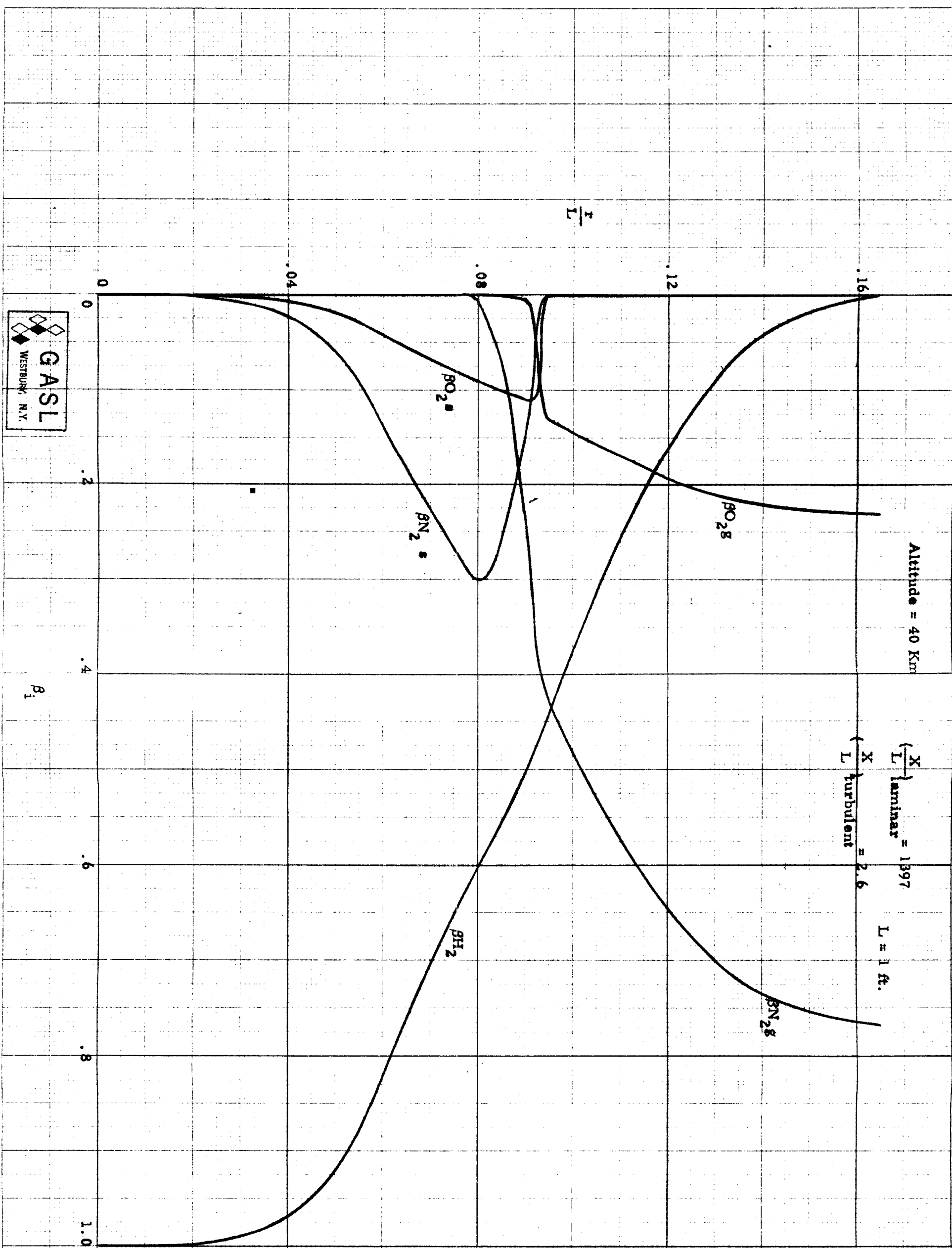


Figure 3a: Radial Distributions of Condensed Phase and Gas Phase Mass Fractions

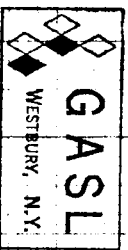
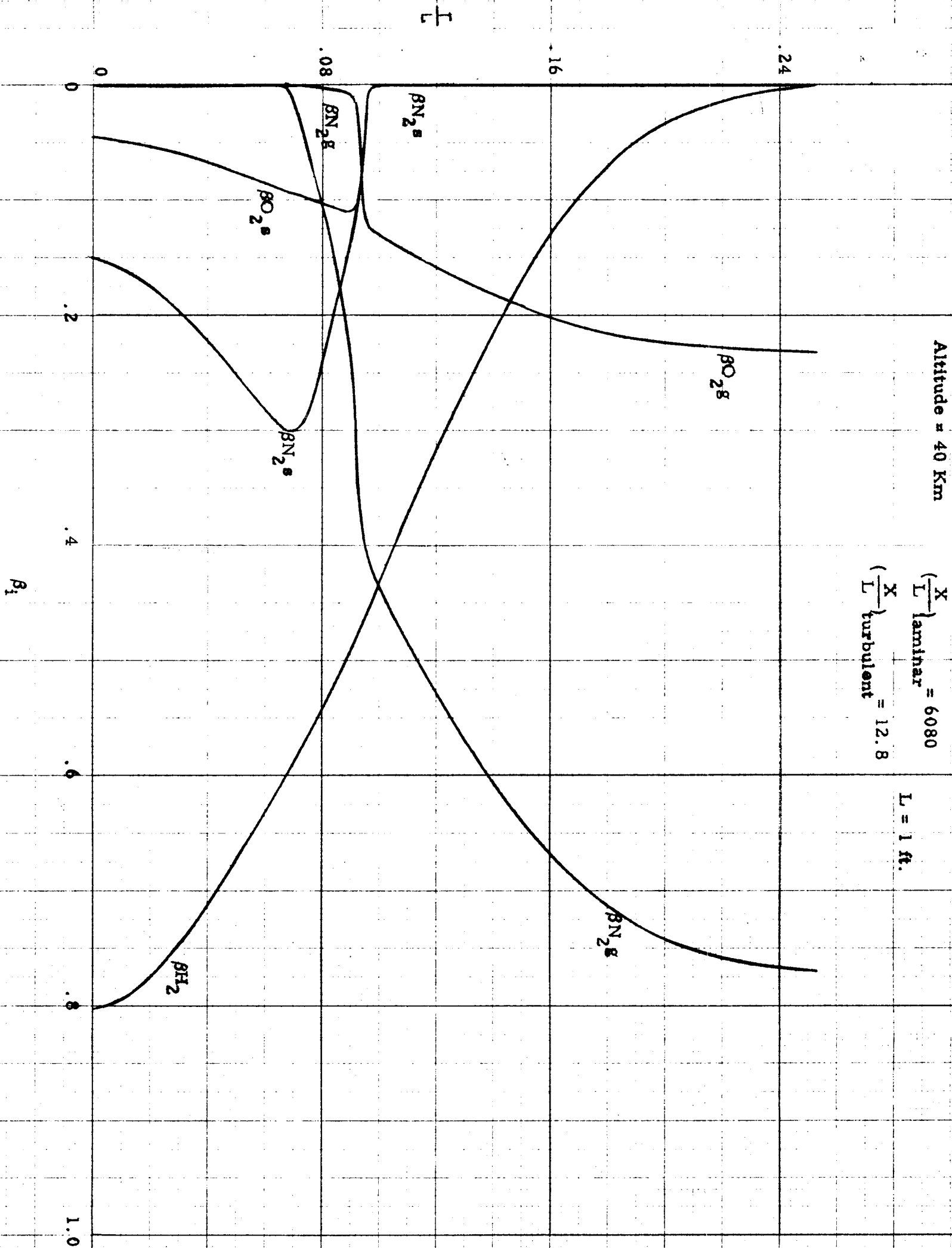


Figure 3b: Radial Distributions of Condensed Phase and Gas Phase Mass Fractions

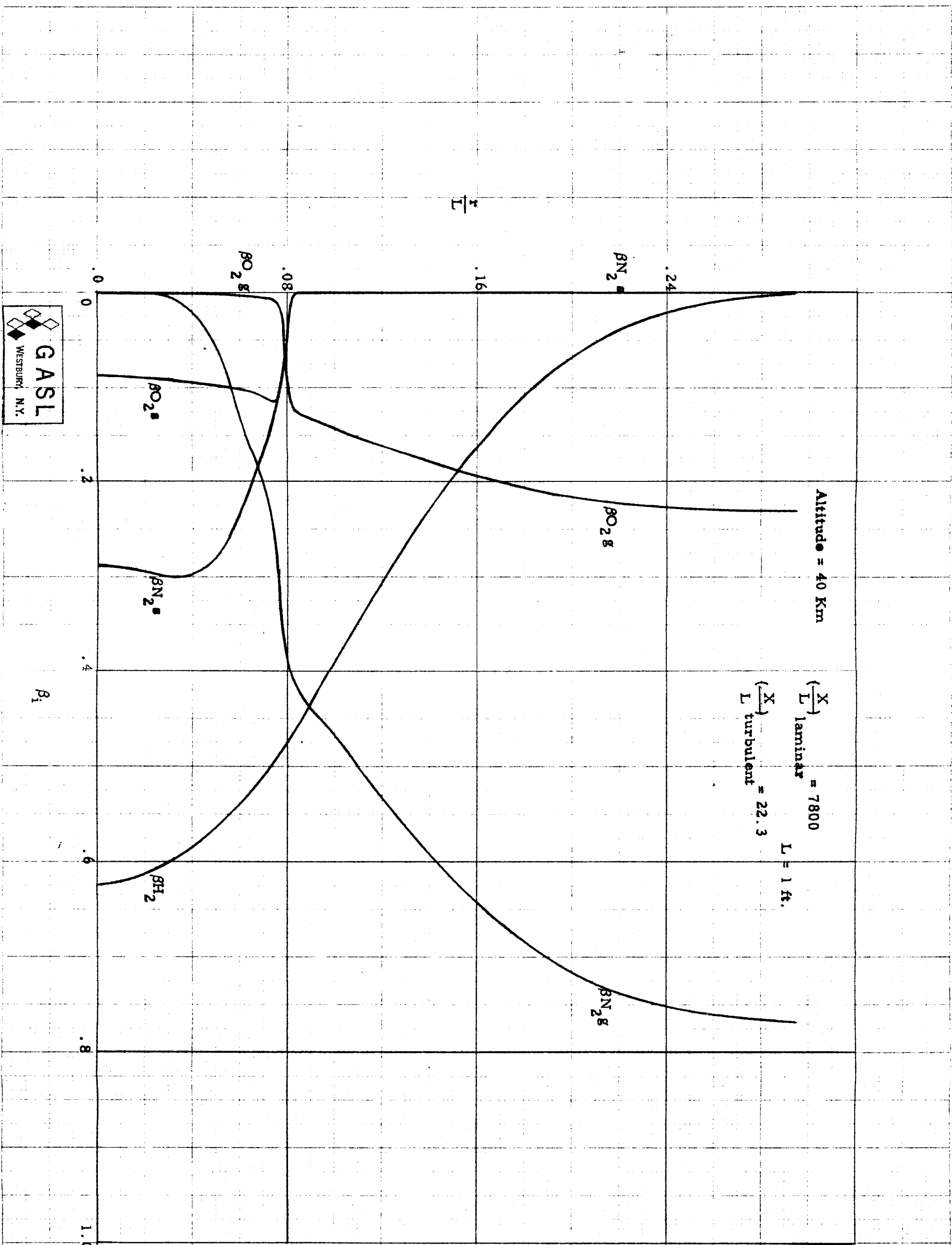


Figure 3c: Radial Distributions of Condensed Phase and Gas Phase Mass Fractions

Figure 3d: Radial Distributions of Velocity
and Temperature at 40 Km

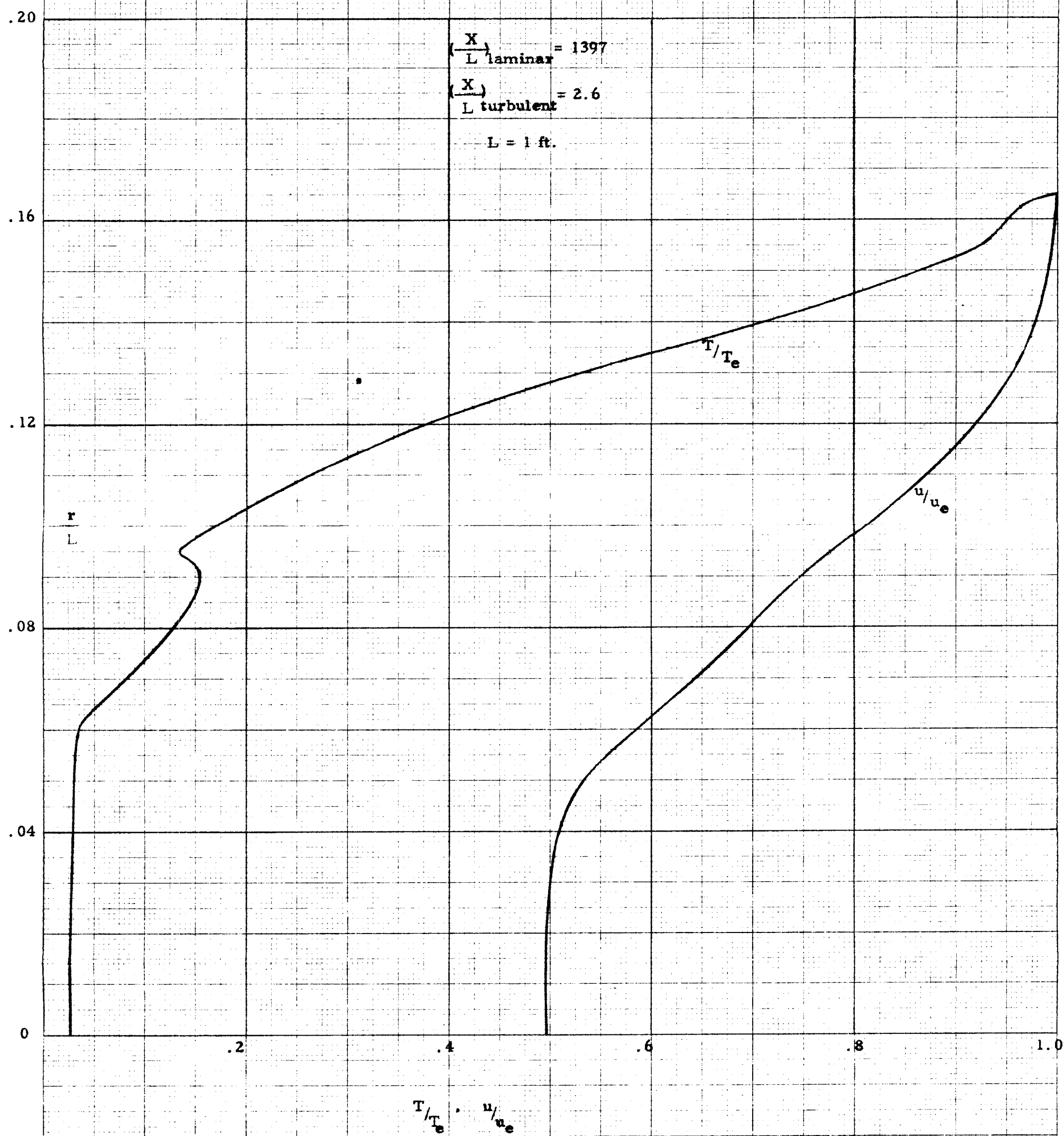


Figure 3e: Radial Distributions of Velocity
and Temperature at 40 Km

$$\left(\frac{X}{L}\right)_{\text{laminar}} = 6080$$

$$\left(\frac{X}{L}\right)_{\text{turbulent}} = 12.8$$

$$L = 1 \text{ ft.}$$

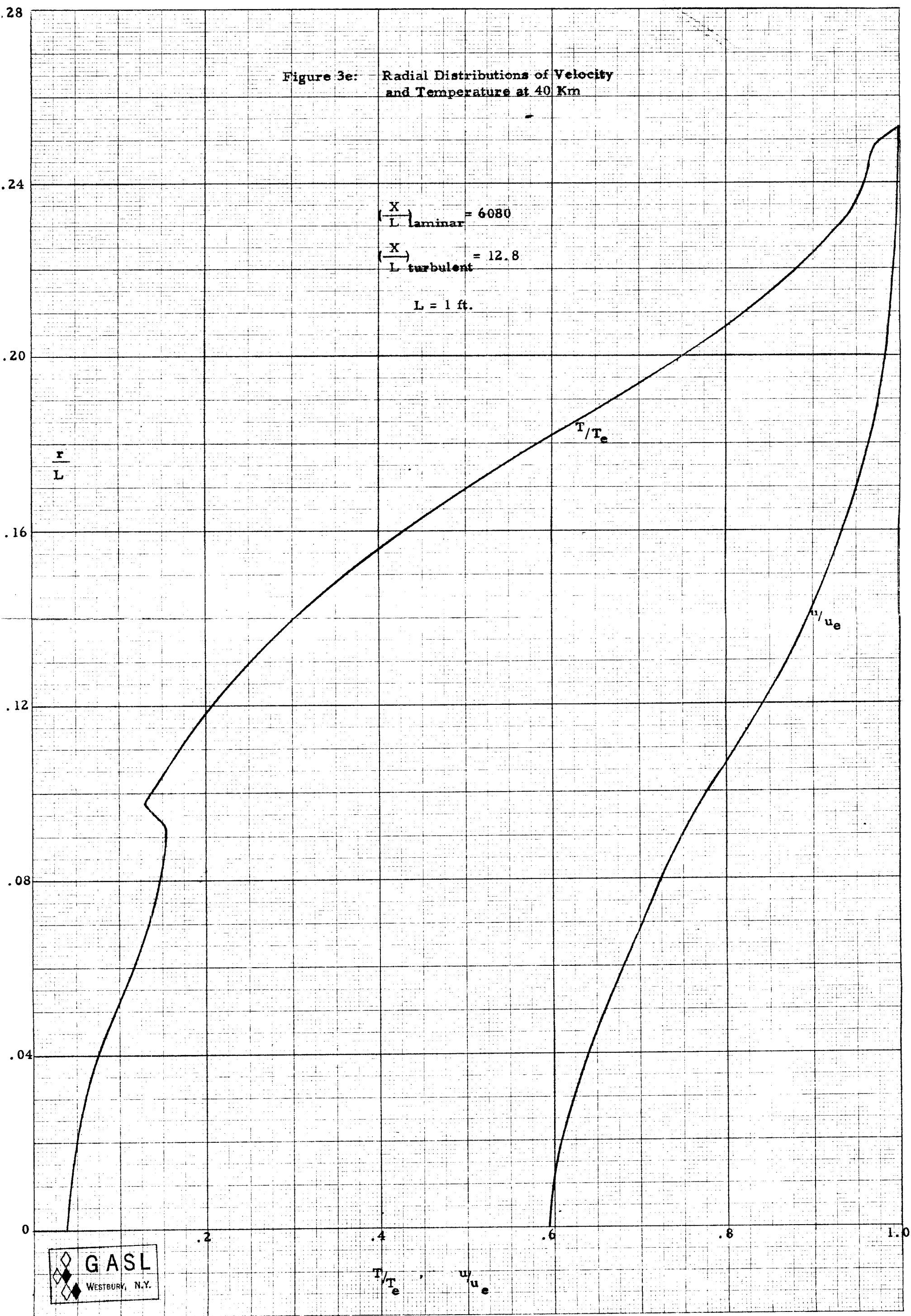


Figure 3f: Radial Distributions of Velocity
and Temperature at 40 Km

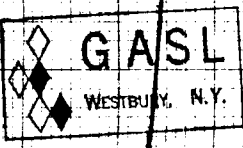
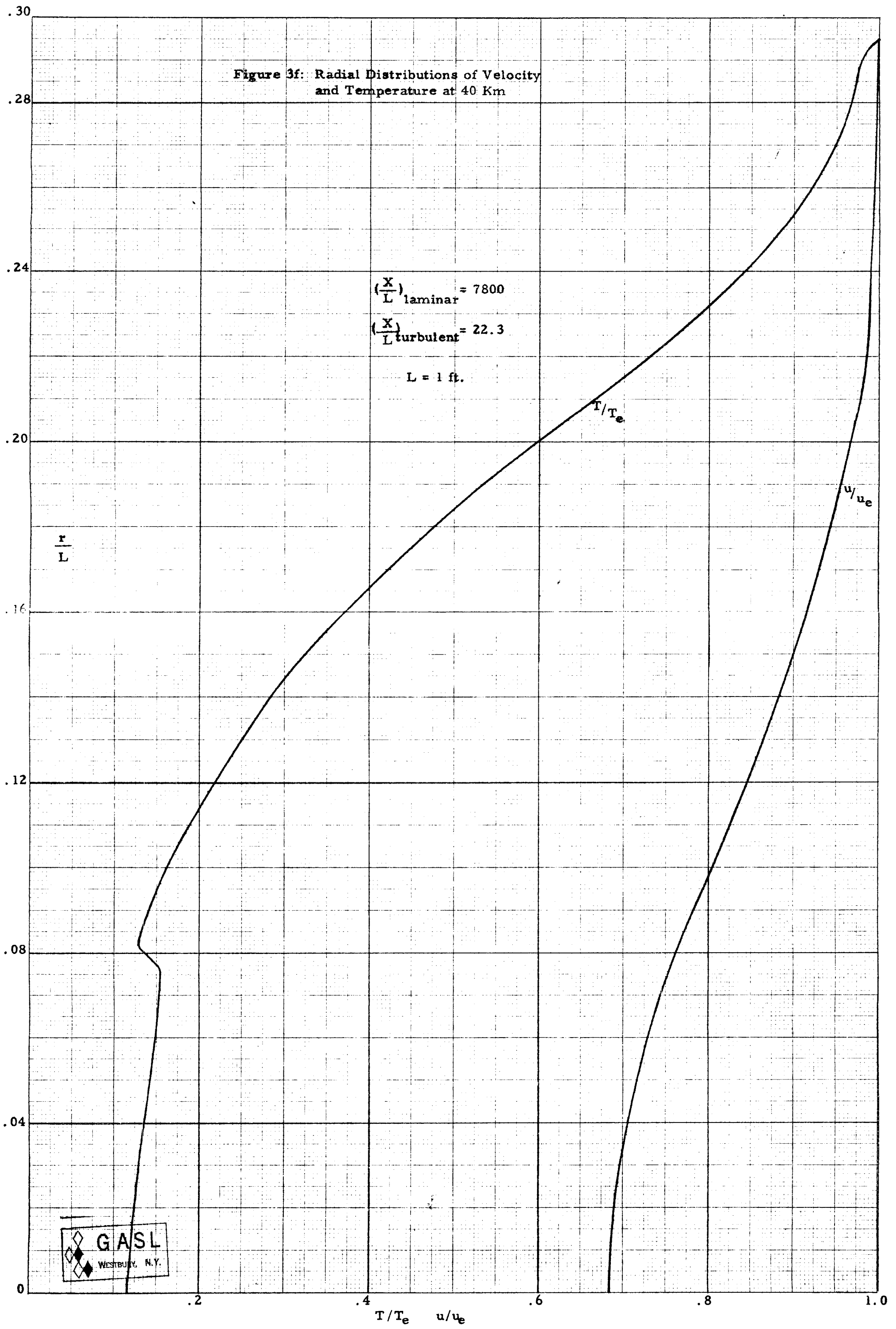


Figure 3: Axial Distribution of Condensed Phase
and Gas Phase Mass Fractions
Laminar Jet = 40 Km

$L = 1 \text{ ft.}$

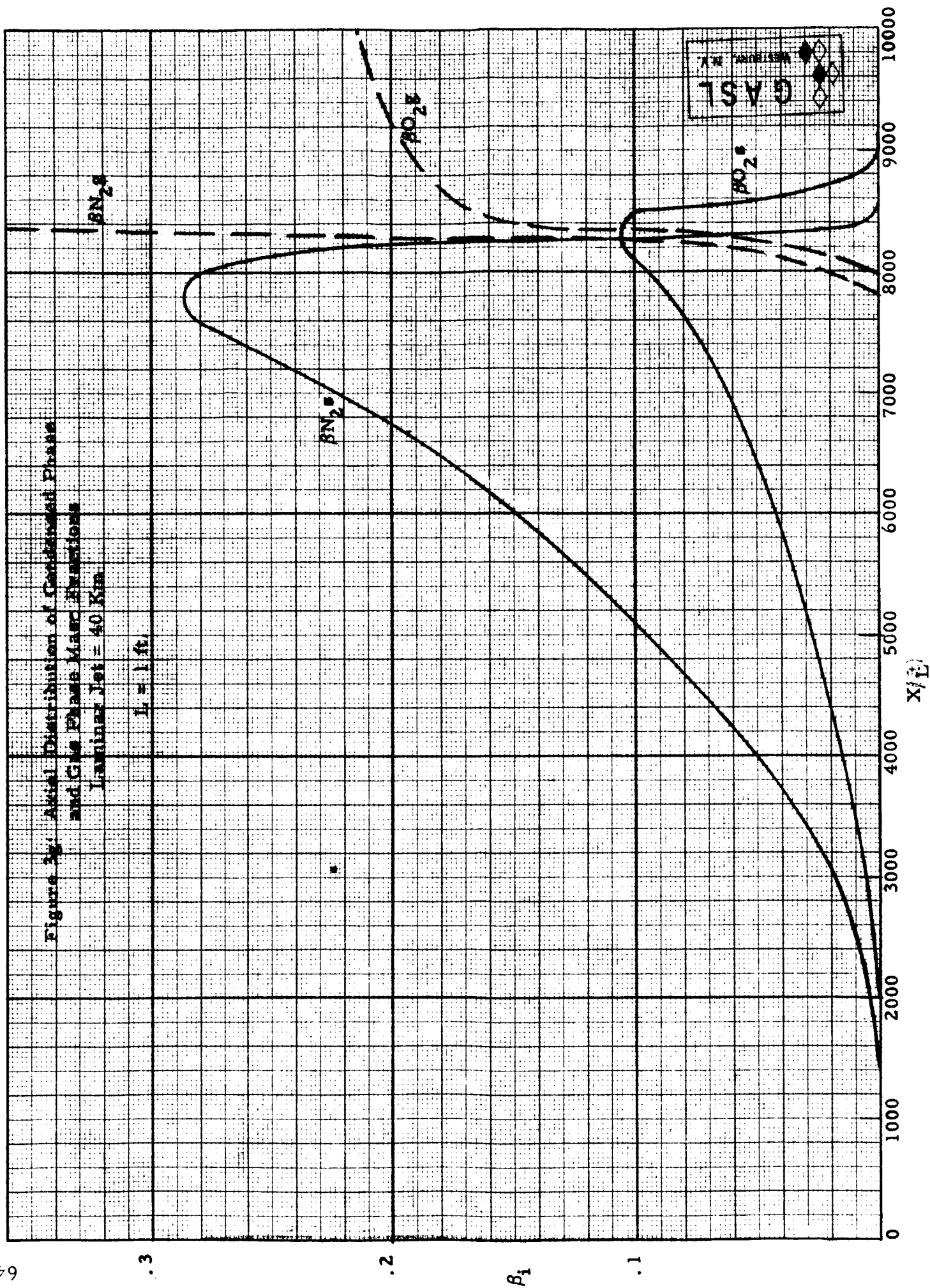
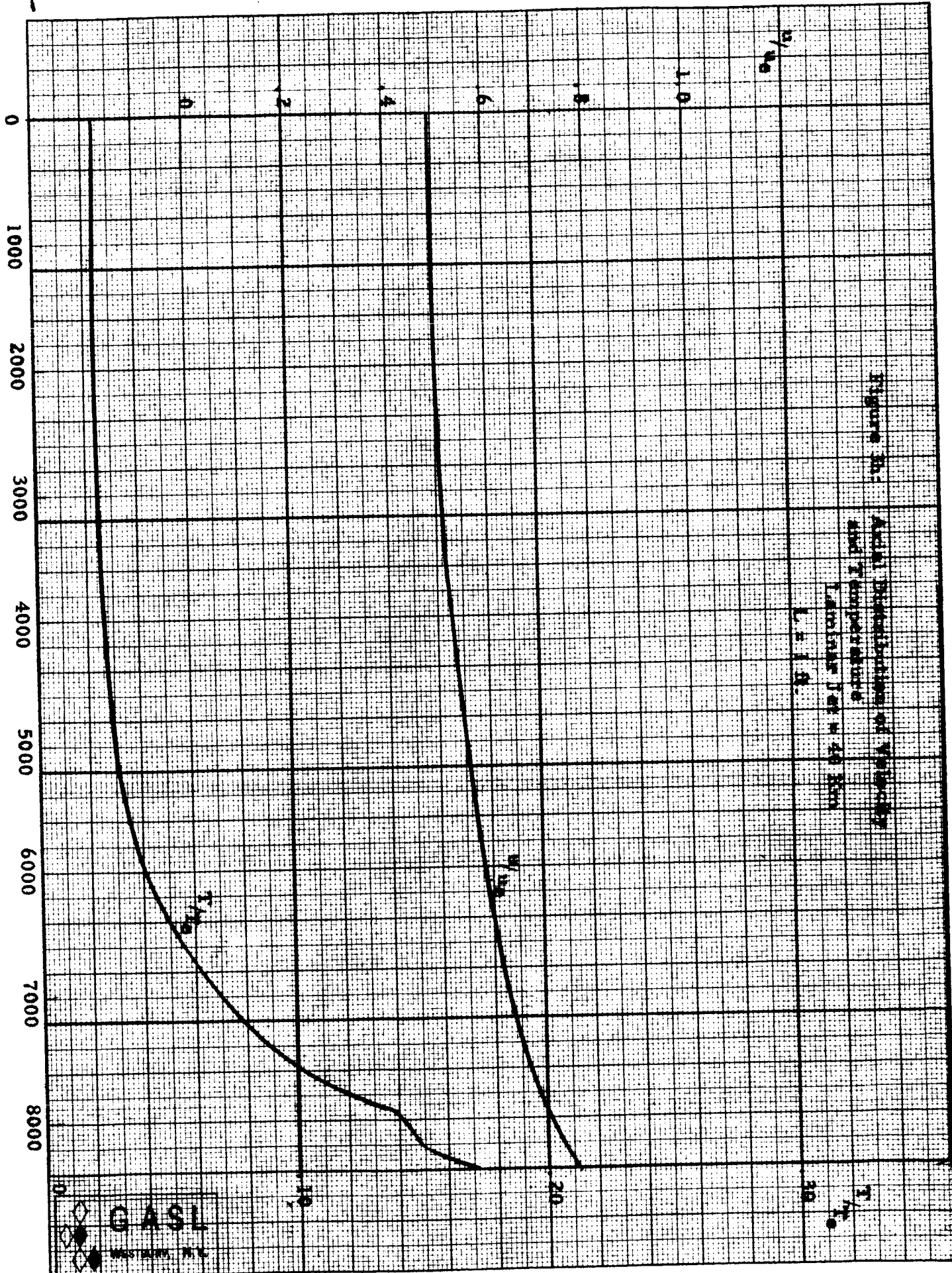


Figure 20:

Acid Distribution of Vapor-
and Temperature
Laminar Jet w 40 mm
 $L = 1.0$.

 x/L


GASL
EUGENE DIETZGEN CO.
MILLIMETER

EUGENE DIETZGEN CO.
SAN FRANCISCO, CALIF.

NO. 340R-10 DIETZGEN GRAPH PAPER
MILLIMETER

Figure 3i: Axial Distributions of Condensed Phase
and Gas Phase Mass Fractions - Turbulent Jet - 40 Km

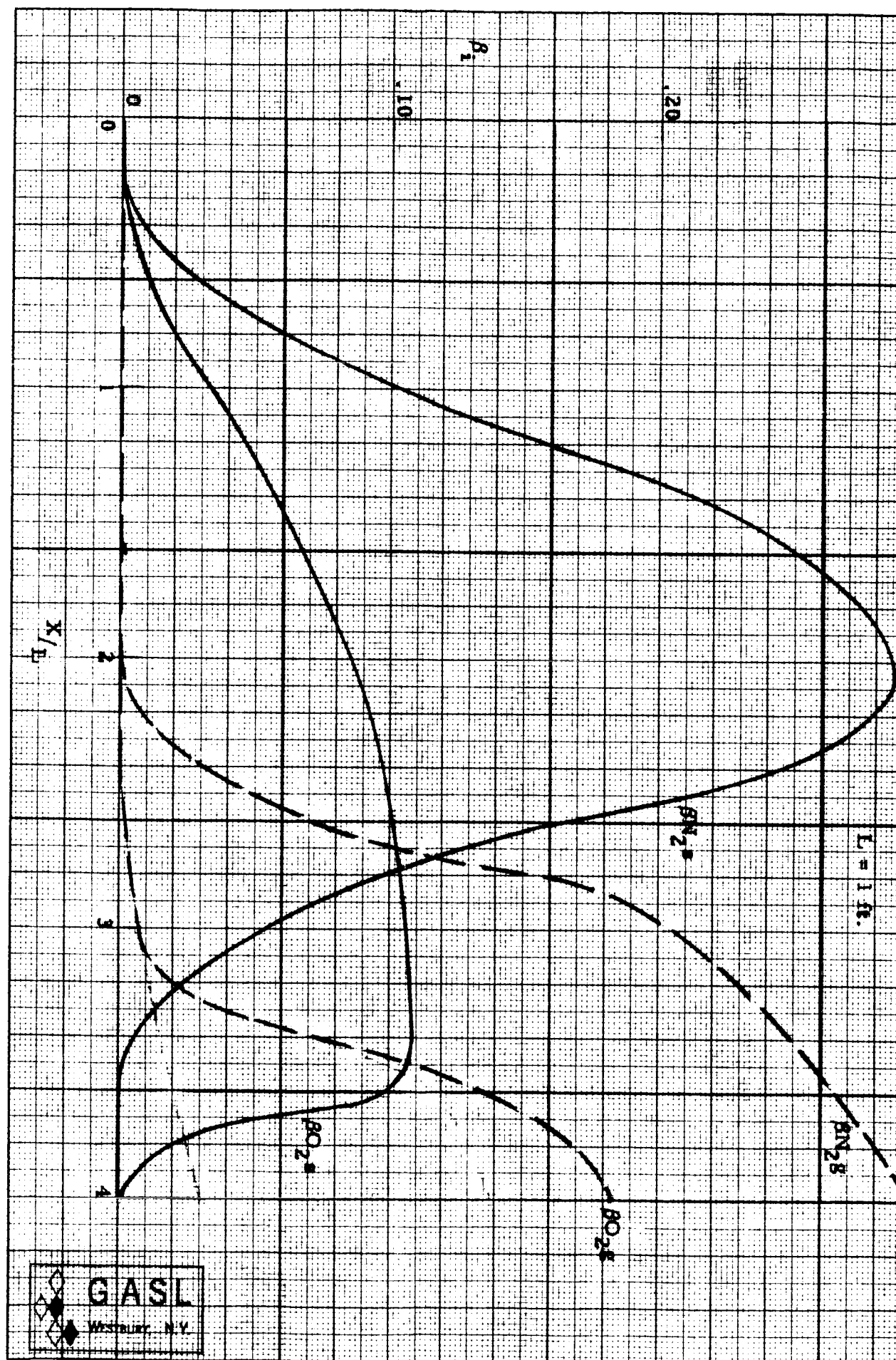
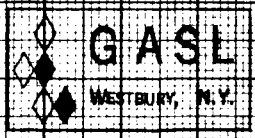
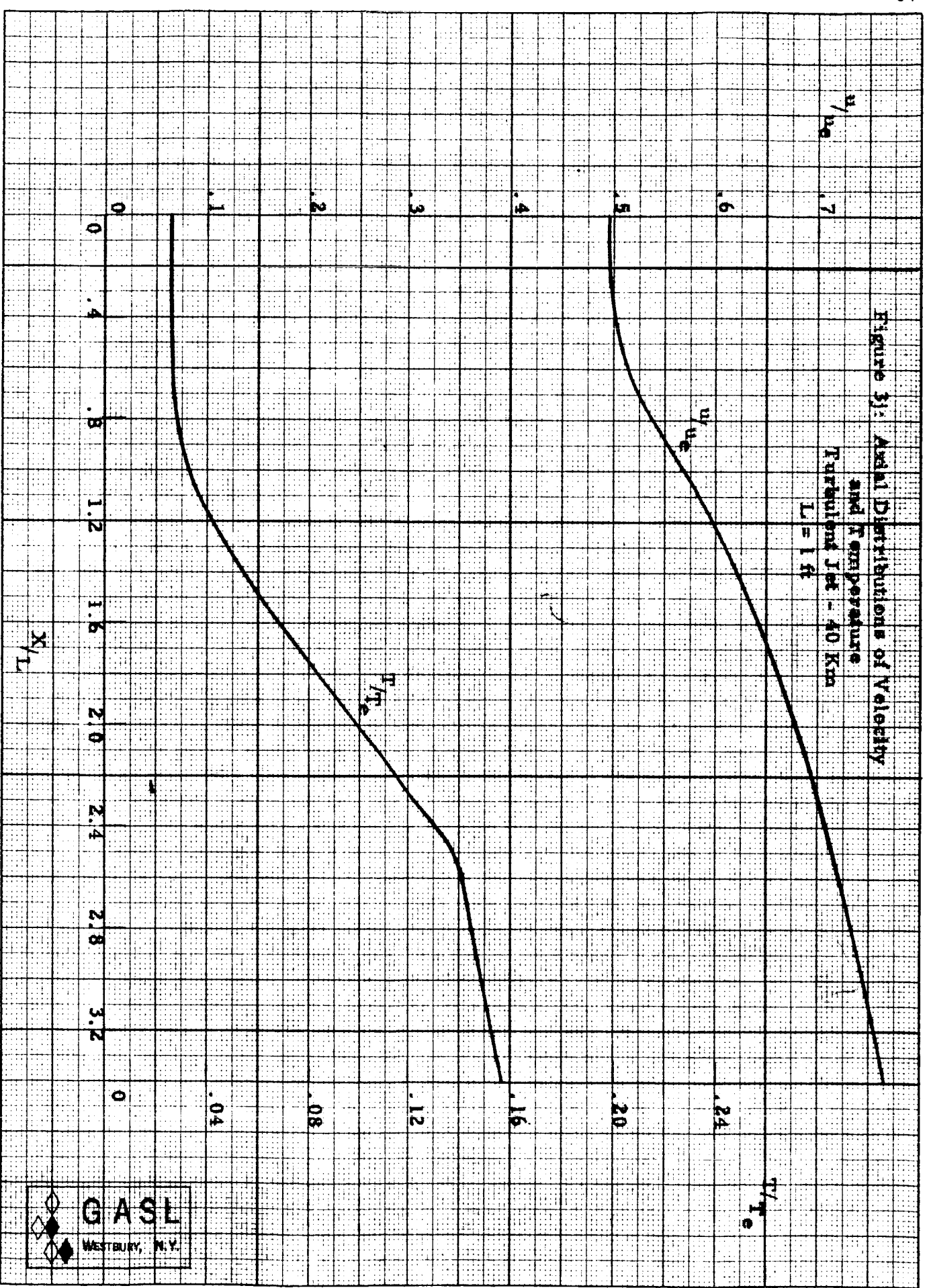


Figure 3: Axial Distributions of Velocity and Temperature

Turbulent Jet - 40 Kpa

$L = 1$ ft



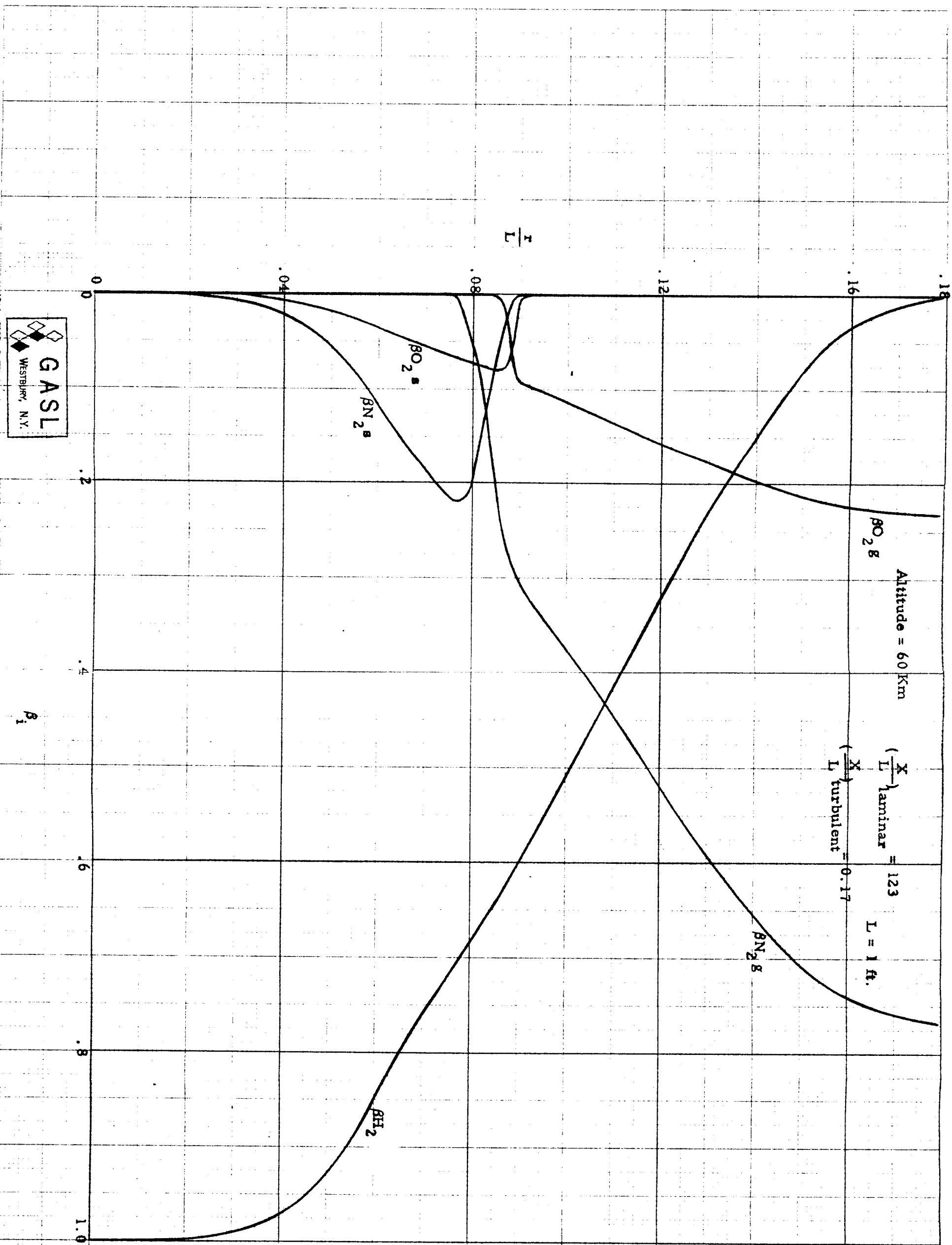


Figure 4a: Radial Distributions of Condensed Phase and Gas Phase Mass Fractions

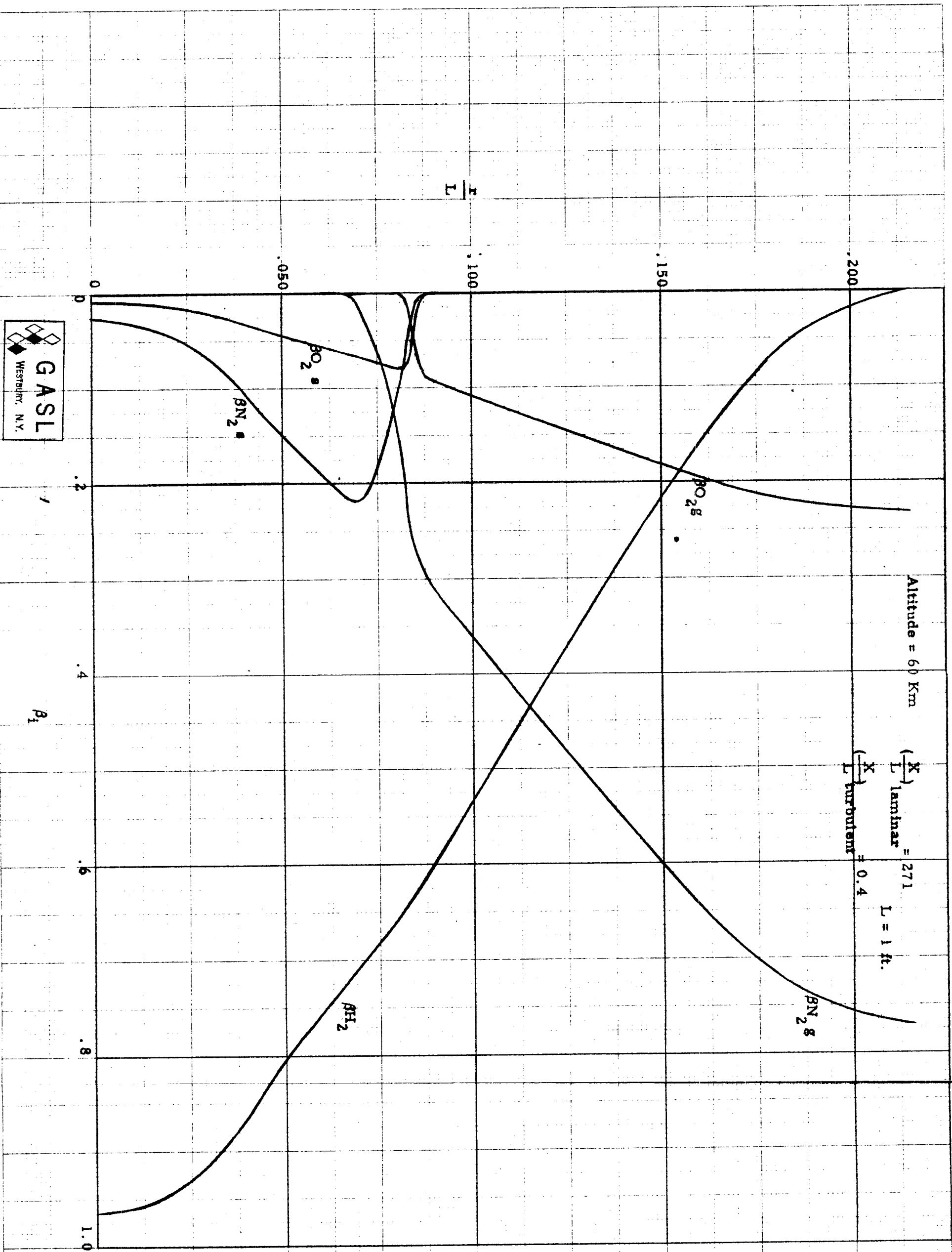
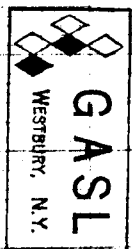
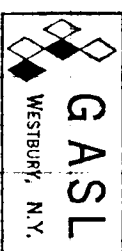


Figure 4b: Radial Distributions of Condensed Phase and Gas Phase Mass Fractions



70

Figure 4d: Radial Distributions of Velocity
and Temperature at 60 Km

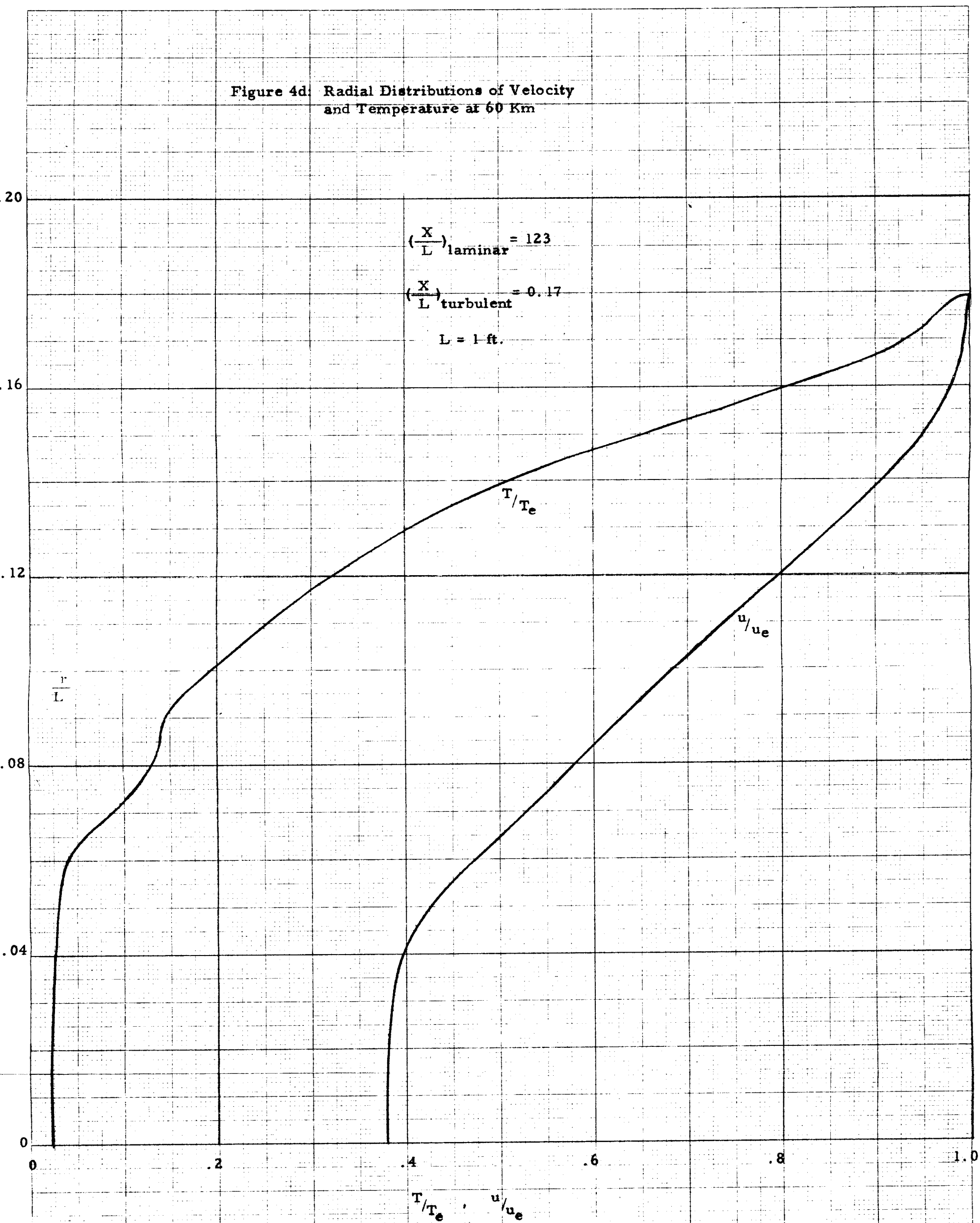


Figure 4e: Radial Distributions of Velocity
and Temperature at 60 Km

$$\left(\frac{X}{L}\right)_{\text{laminar}} = 276$$

$$\left(\frac{X}{L}\right)_{\text{turbulent}} = 0.40$$

$$L = 1 \text{ ft.}$$

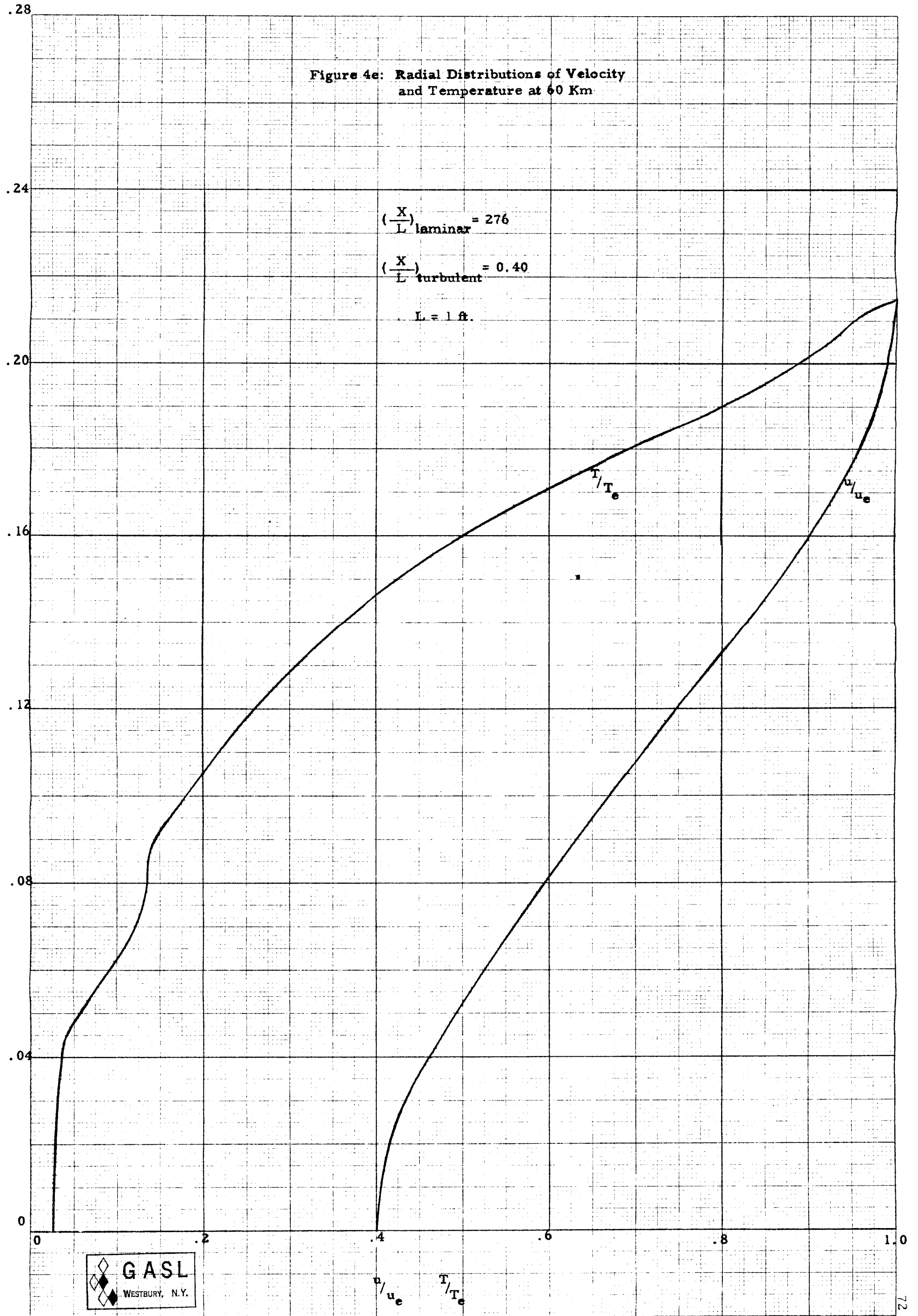


Figure 4f: Radial Distributions of Velocity
and Temperature at 60 Km

$$\left(\frac{X}{L}\right)_{\text{laminar}} = 443$$

$$\left(\frac{X}{L}\right)_{\text{turbulent}} = 0.08$$

$$L = 1 \text{ ft.}$$

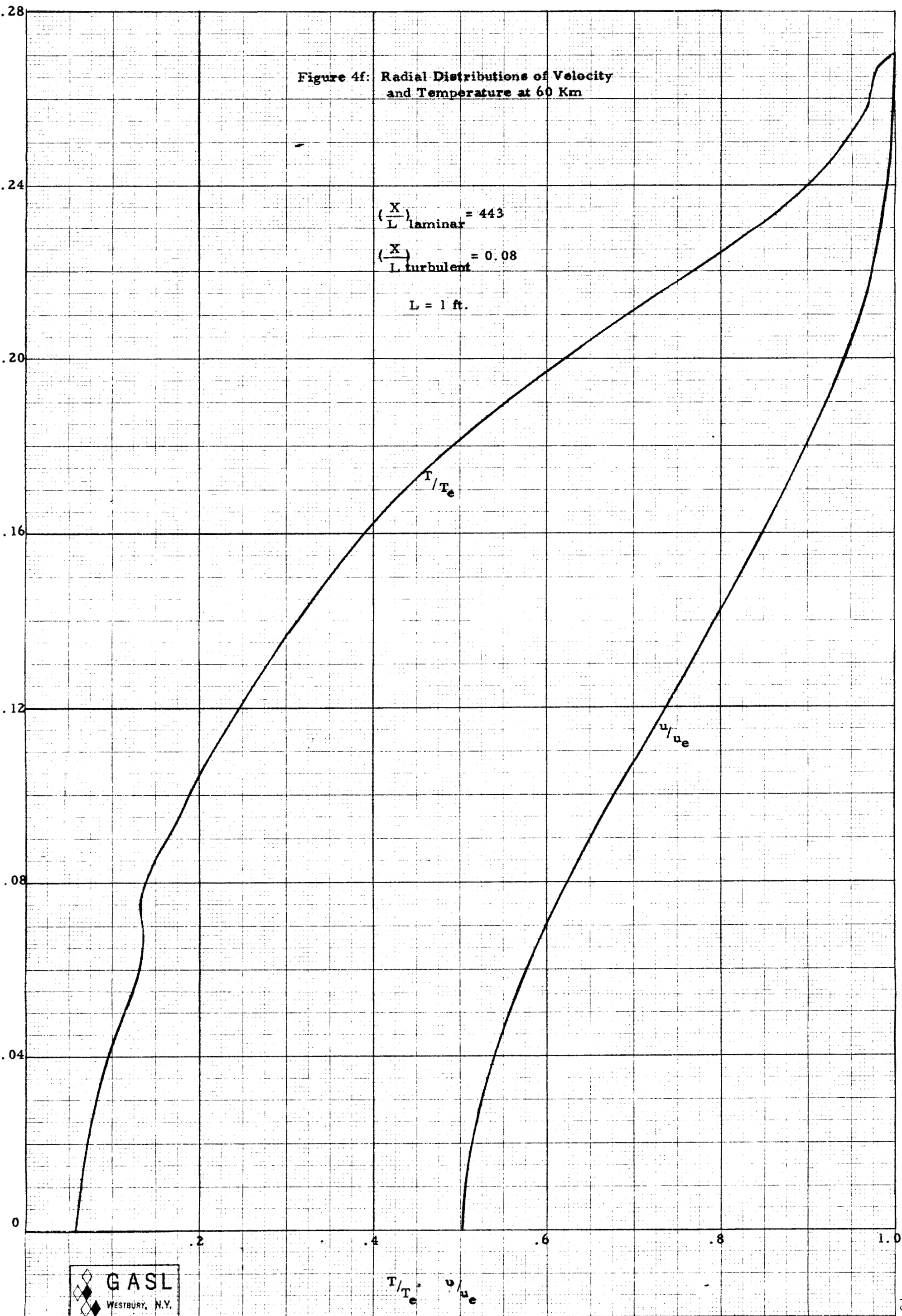
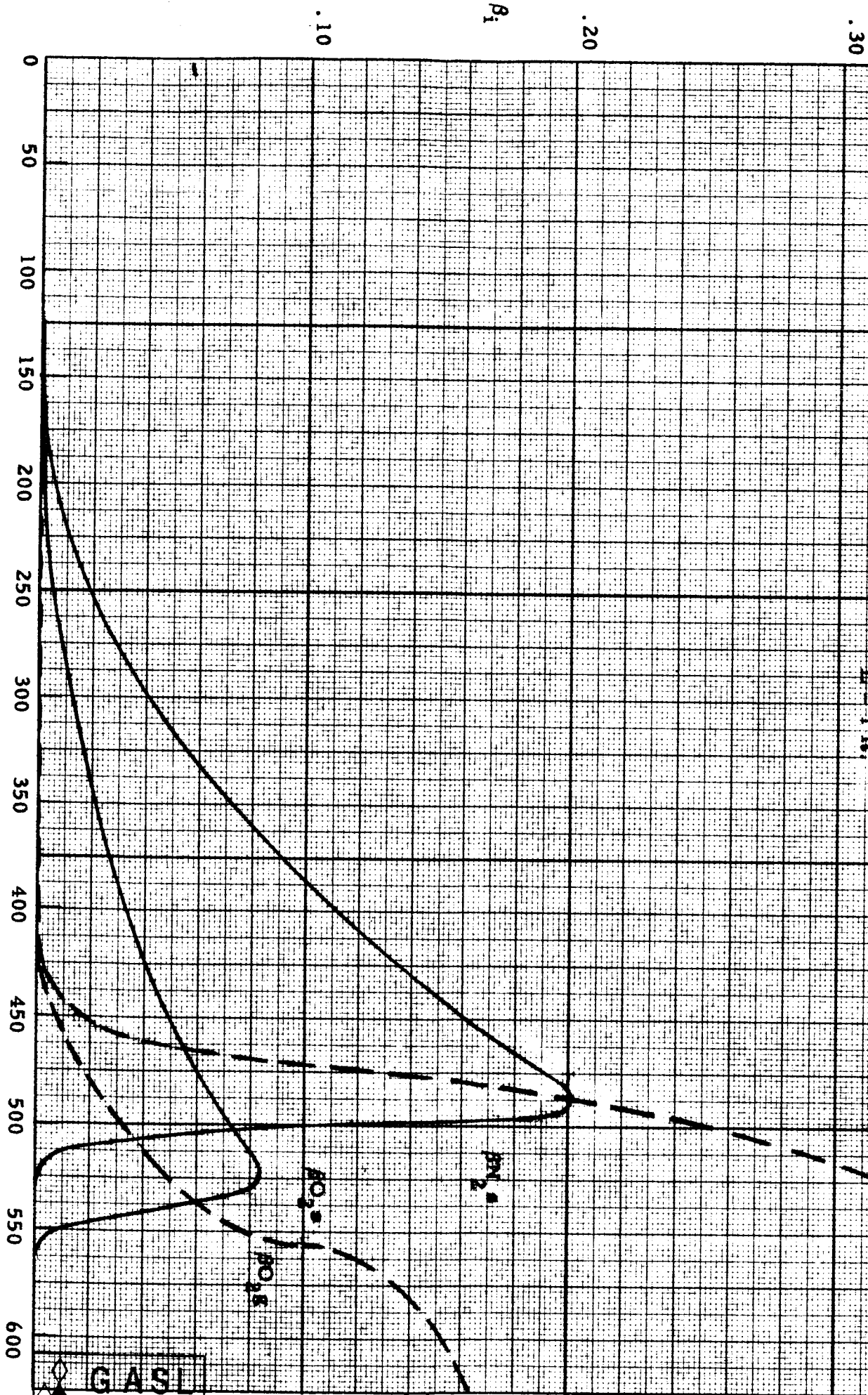


Figure 4g: Axial Distributions of Condensed Phase
and Gas Phase Mass Fractions
Laminar Jet - 60 KPa

$L = 1$ ft.



GAS

WESTBURY, N.Y.

Figure 4h: Axial Distributions of Velocity and Temperature - Turbulent Jet - 60 KHz

Figure 4b: Distributions of Velocity
and Temperature
Laminar Jet - 60 Km

$L = 1 \text{ ft.}$

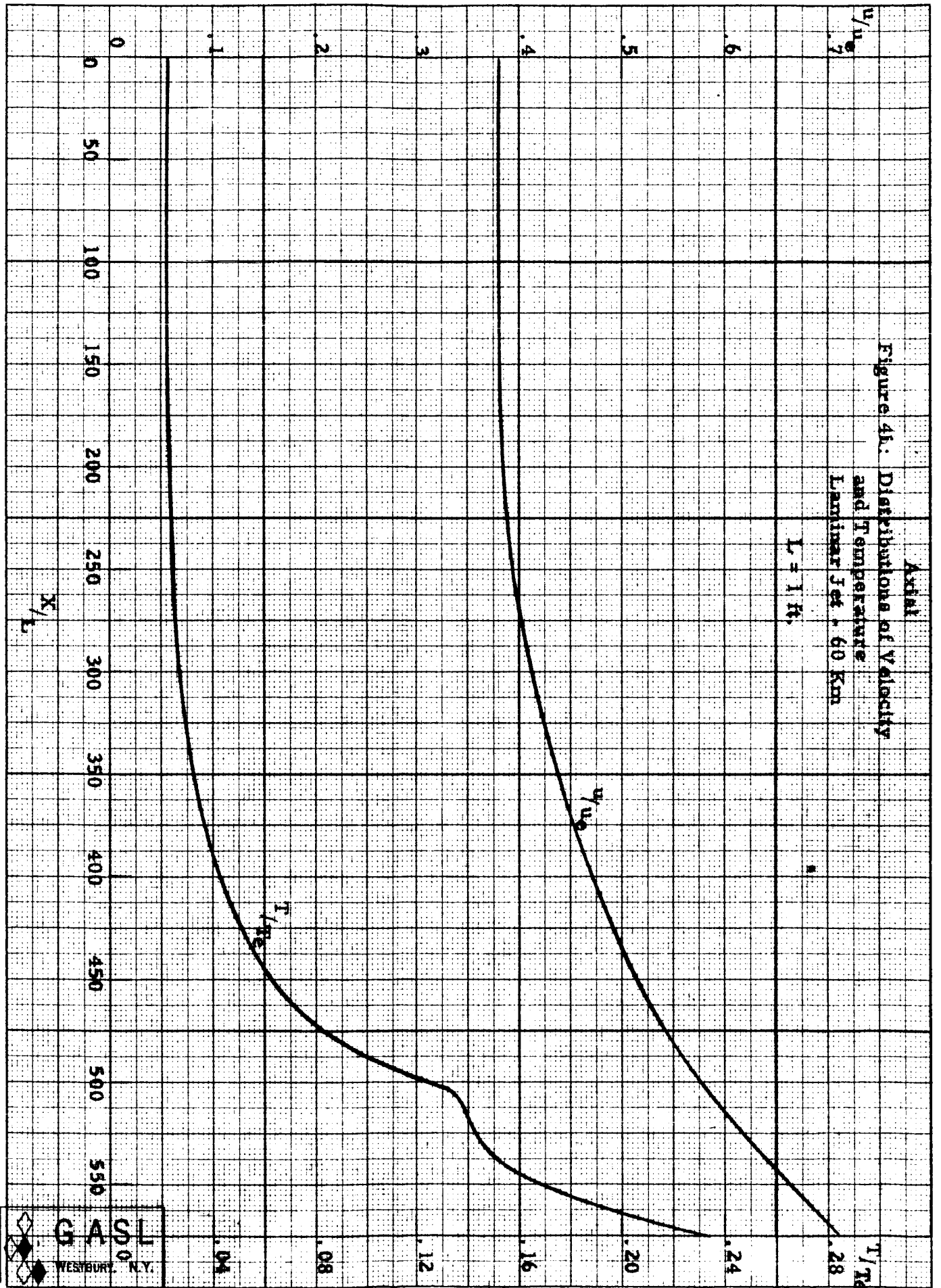
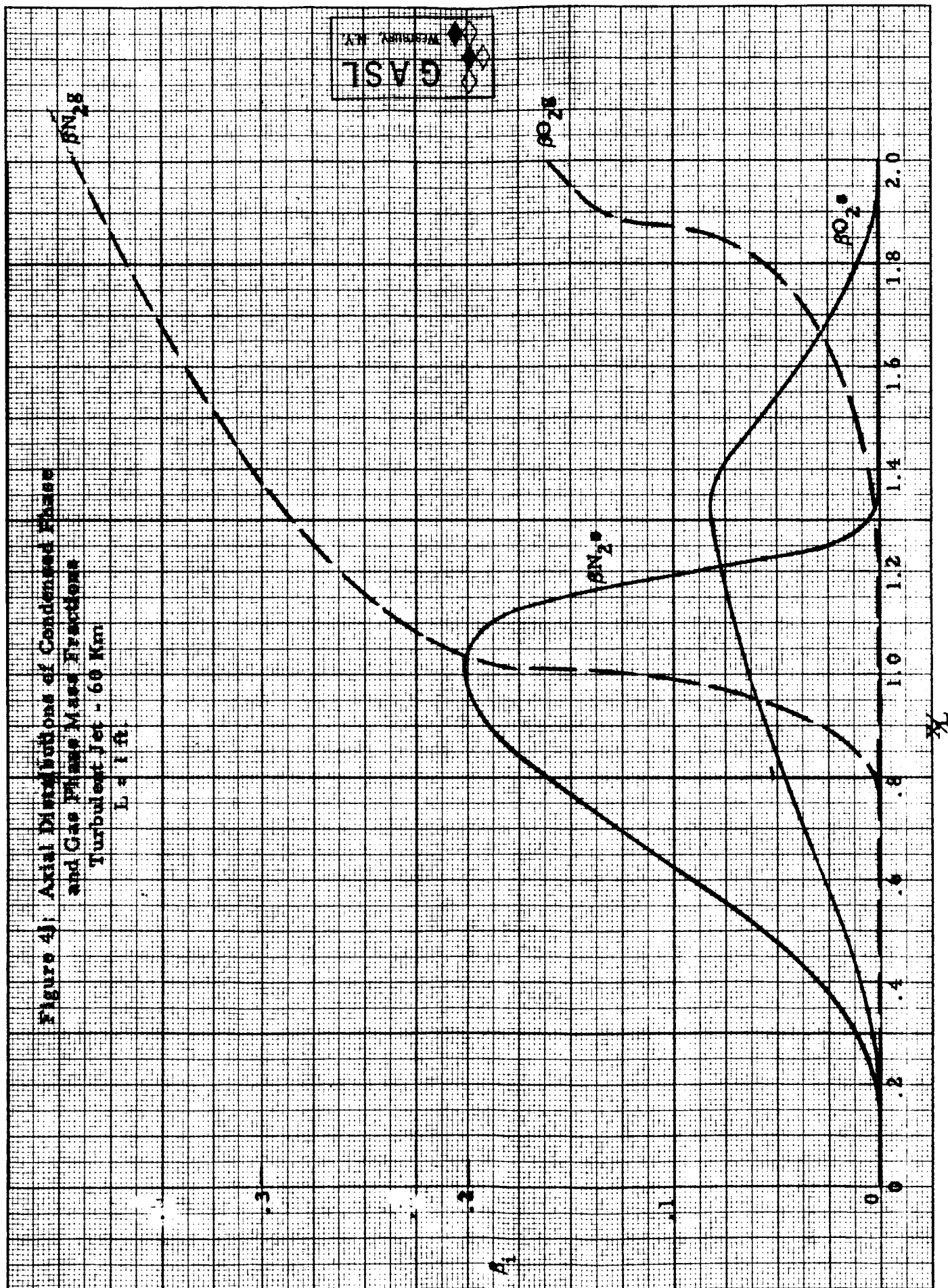


Figure 4): Axial Distributions of Condensed Phase
and Gas Phase Mass Fractions
Turbulent Jet - 60 Km
L = 1 ft.



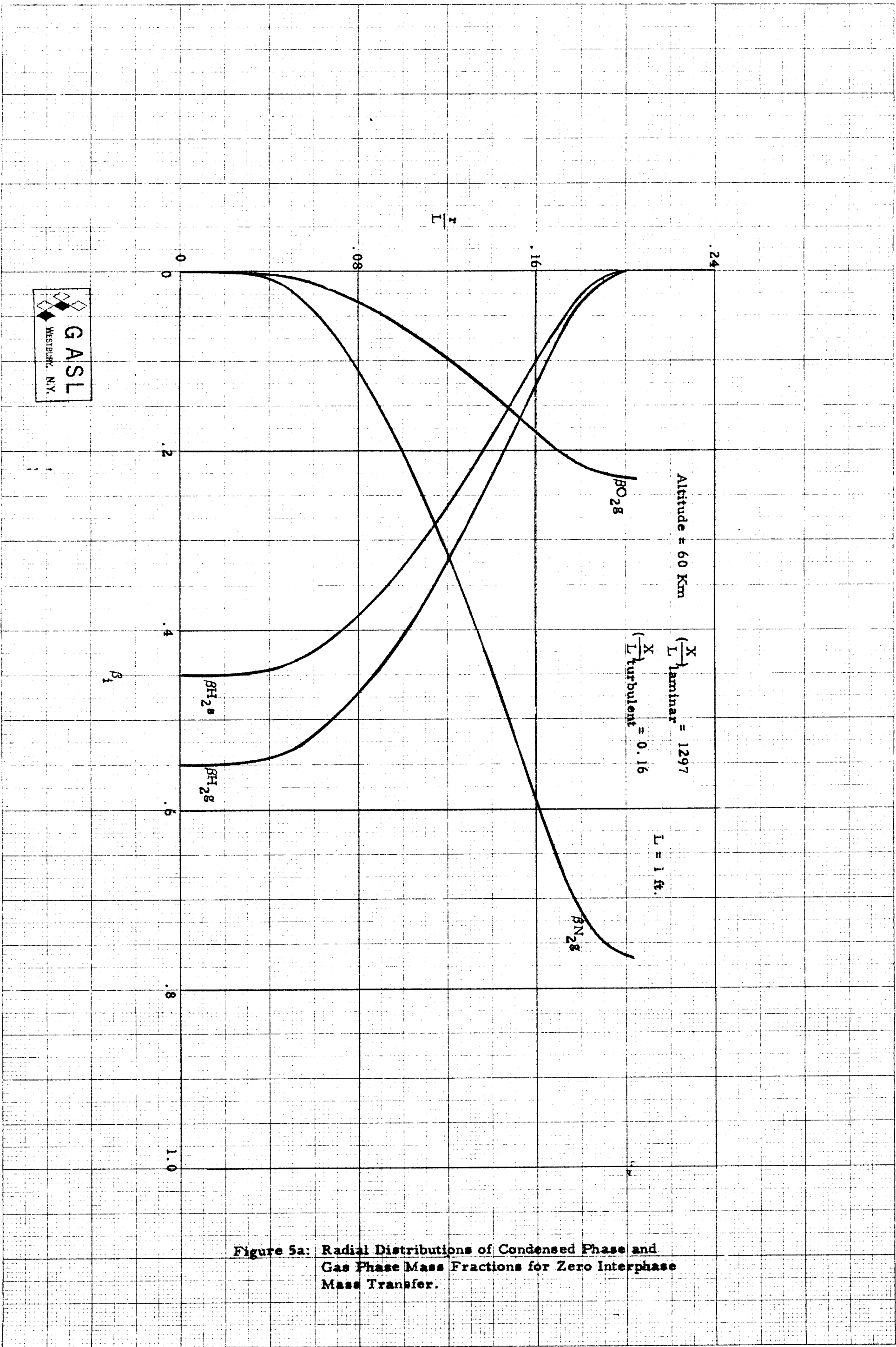


Figure 5a: Radial Distributions of Condensed Phase and Gas Phase Mass Fractions for Zero Interphase Mass Transfer.

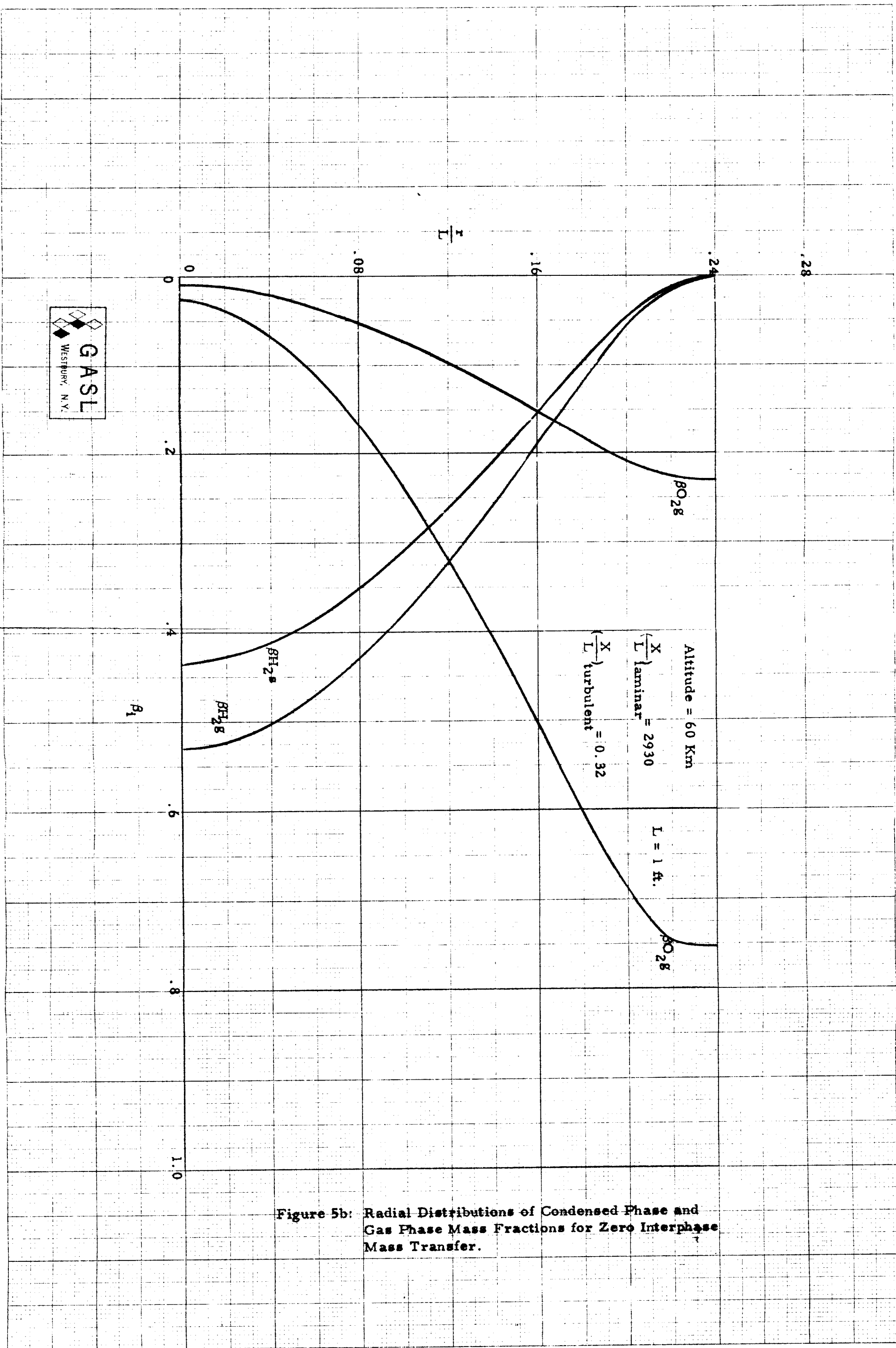
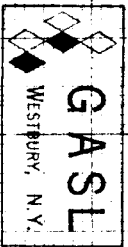


Figure 5b: Radial Distributions of Condensed Phase and Gas Phase Mass Fractions for Zero Interphase Mass Transfer.



NOT BE USED FOR REPRODUCTION OF THIS DOCUMENT

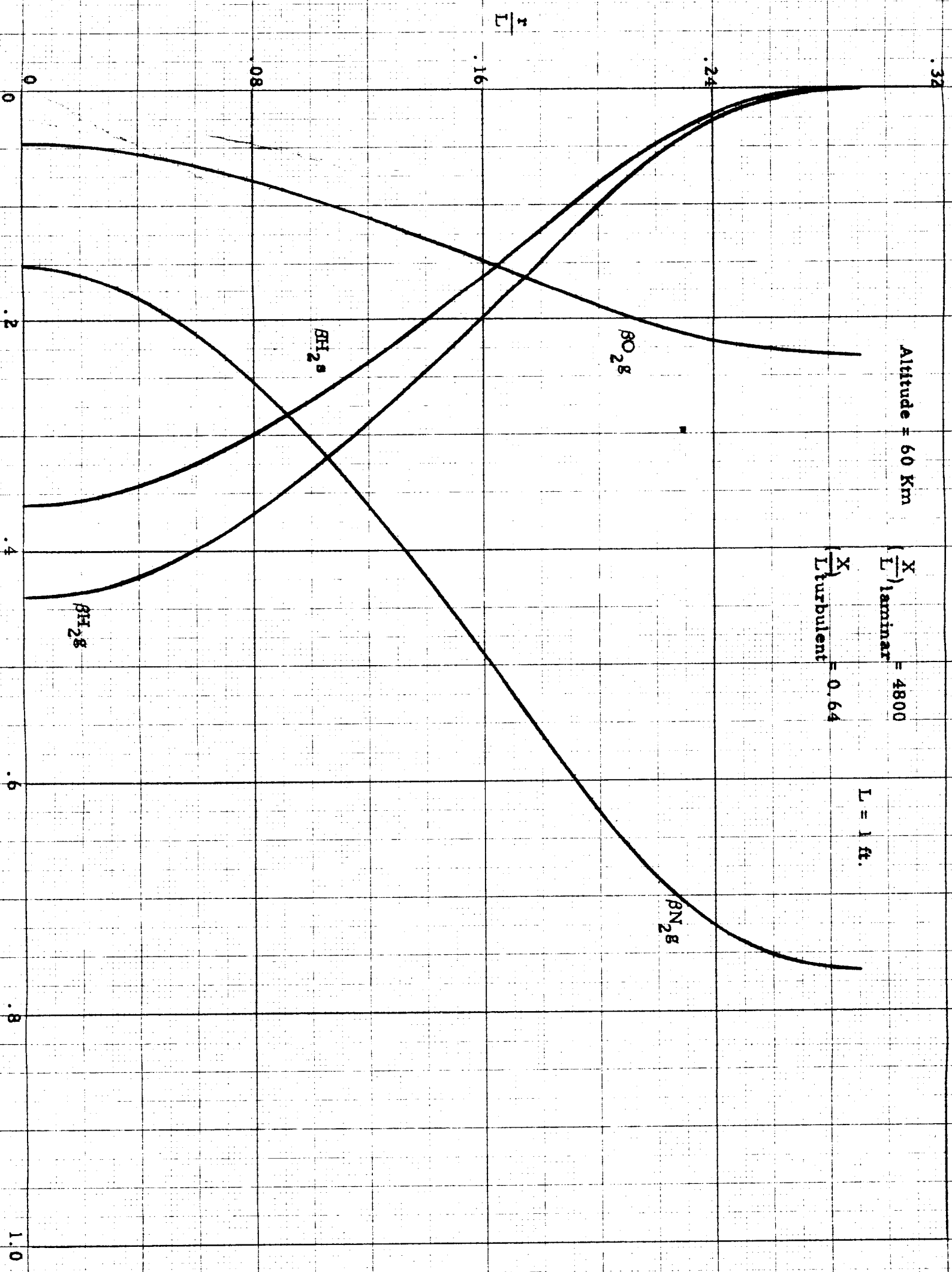
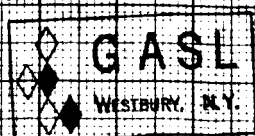
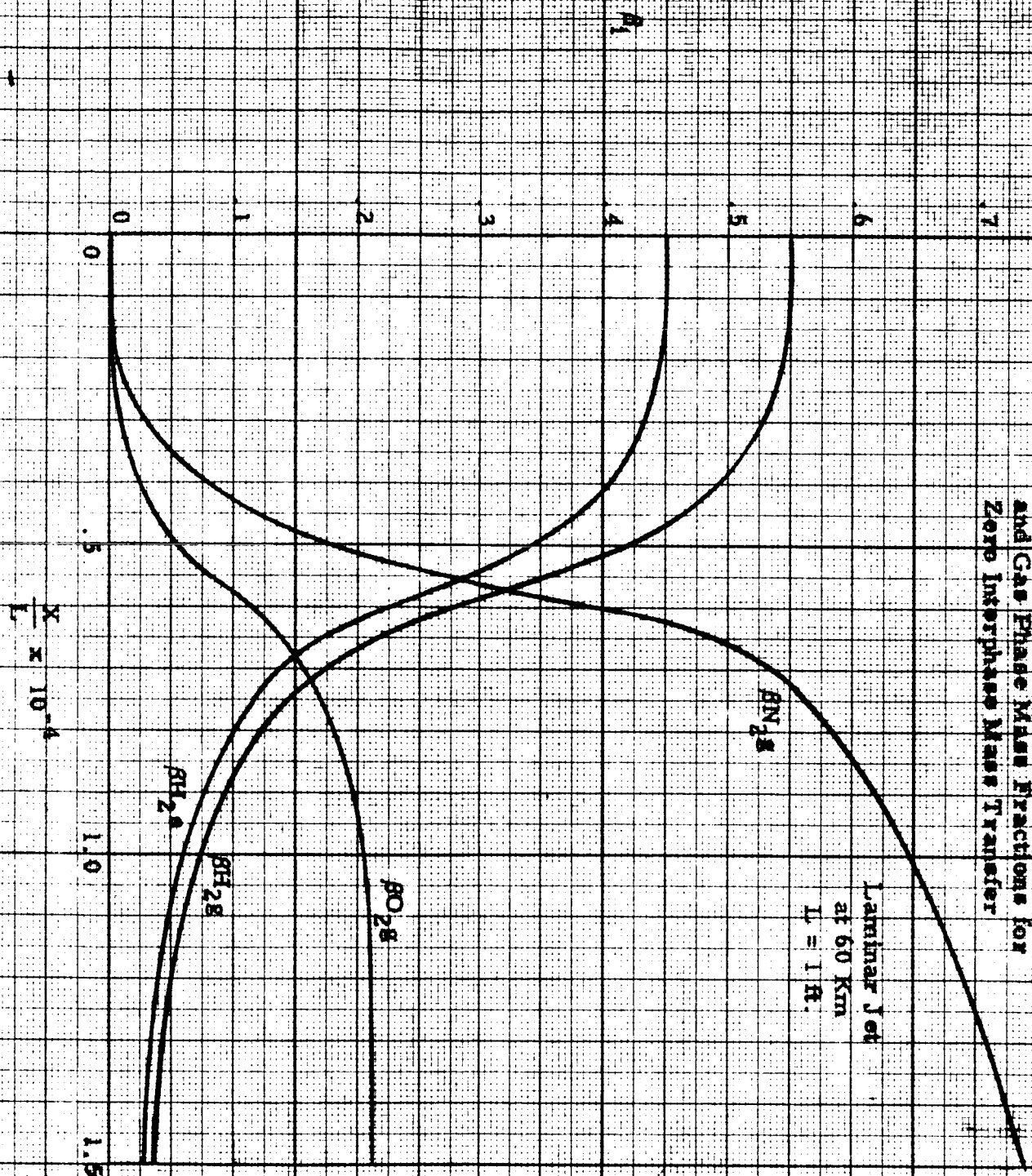


Figure 5c: Radial Distributions of Condensed Phase and Gas Phase Mass Fractions for Zero Interphase Mass Transfer.

Figure 5d: Axial Distributions of Condensed Phase and Gas Phase Mass Fractions for Zero Interphase Mass Transfer



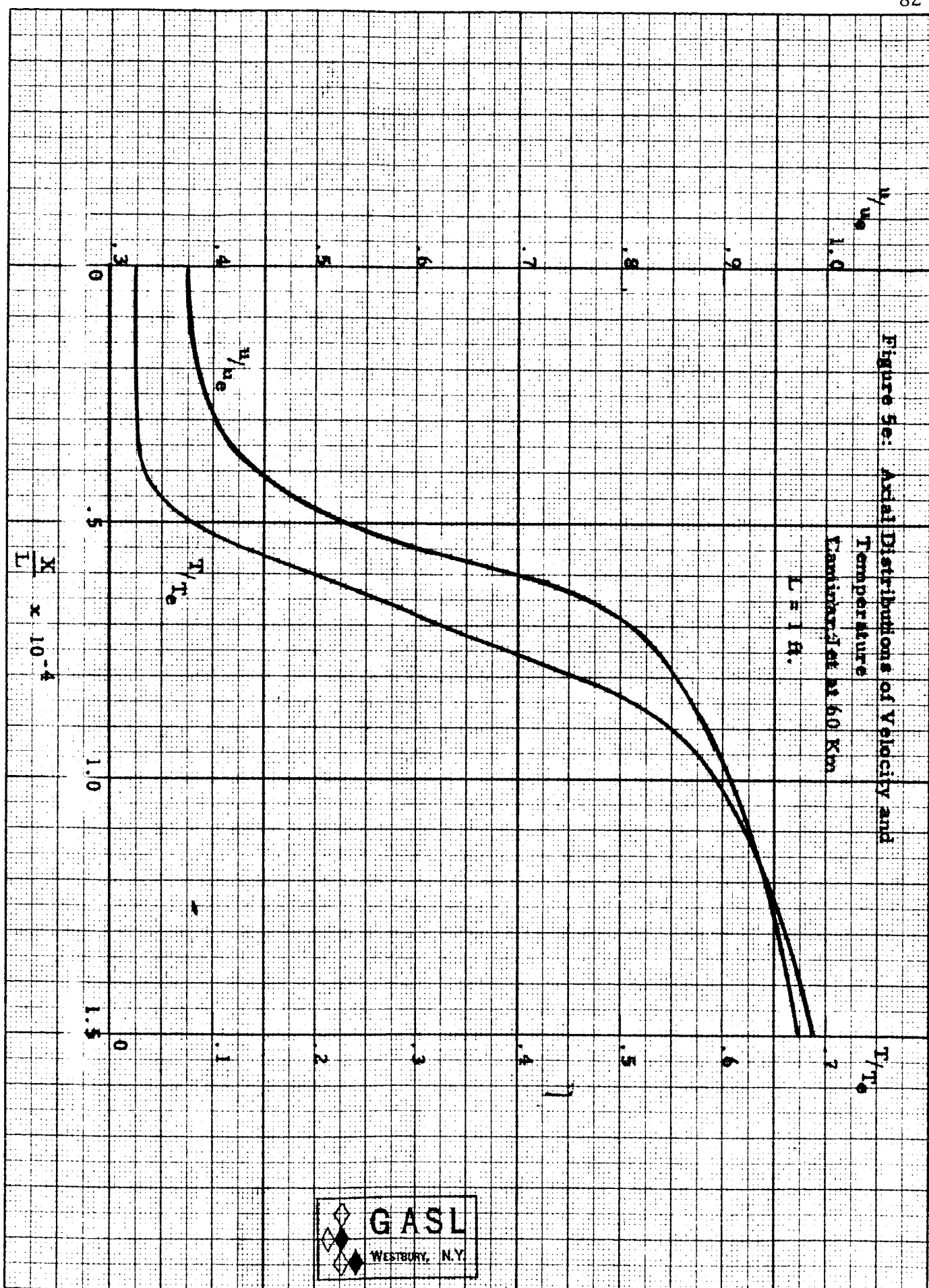


Figure 5f. Axial Distributions of Condensed Phase and Gas Phase Mass Fractions for Zero Interphase Mass Transfer

